3-22-2012

Structural Health Monitoring of M1114 High Mobility Multipurpose Wheeled Vehicle Armor System

Frank T. Sha

Follow this and additional works at: https://scholar.afit.edu/etd

Part of the Materials Science and Engineering Commons

STRUCTURAL HEALTH MONITORING OF M1114 HIGH MOBILITY MULTIPURPOSE WHEELED VEHICLE ARMOR SYSTEM

THESIS

FRANK T.J. SHA, CAPTAIN, USAF

AFIT/GEM/ENV/12-M19

DEPARTMENT OF THE AIR FORCE
AIR UNIVERSITY

AIR FORCE INSTITUTE OF TECHNOLOGY

Wright-Patterson Air Force Base, Ohio

AFIT/GEM/ENV/12-M19

STRUCTURAL HEALTH MONITORING OF M1114 HIGH MOBILITY
MULTIPURPOSE WHEELED VEHICLE ARMOR SYSTEM

THESIS

Presented to the Faculty

Department of Systems and Engineering Management

Graduates School of Engineering and Management

Air Force Institute of Technology

Air University

Air Education and Training Command

In Partial Fulfillment of the Requirements for the

Degree of Master of Science in Engineering Management

Frank T.J. Sha, Captain

March 2012

AFIT/GEM/ENV/12-M19

STRUCTURAL HEALTH MONITORING OF M1114 HIGH MOBILITY
MULTIPURPOSE WHEELED VEHICLE ARMOR SYSTEM

Frank T.J. Sha, BS
Captain, USAF

Approved:

//signed//	2 March 2012
Som Soni, PhD, Chair	Date

//signed//	2 March 2012
Alfred E. Thal Jr., PhD, Member	Date

//signed//	2 March 2012
James L. Blackshire, PhD, Member (AFRL/NDE)	Date

AFIT/GEM/ENV/12-M19

Abstract

The M1114 High Mobility Multipurpose Wheeled Vehicle (HMMWV) has been
the workhorse vehicle of the United States Armed Forces in Afghanistan and Iraq.
Donald Rumsfeld, Secretary of Defense, was faced with massive public criticism in 2004,
for not equipping our military personnel in Afghanistan and Iraq with M1114 with the
proper ballistic armor. In May 2004, a $618M Senate Bill was passed to increase
production level of HMMWV's and improve the ballistic protection capabilities while
minimizing additional weight. While the military is taking advantages using composite
armor on a HMMWV, the military does not have a rigorous method to detect, locate, and
to quantify damage on a two layer composite armor system.

Structural Health Monitoring (SHM) is the process of implementing a damage
detection and characterization strategy for engineering structures. Damage is defined as
changes to the material and geometric properties of a structural system, including
changes to the boundary conditions and system connectivity, which adversely affect the
system's performance. An active SHM system was developed to detect, locate, and
quantify for damage on a two layer composite armor (HJ1 composite with ceramic frontal
plates) potentially encountering impact from a 0.30 caliber armor piercing projectile.

An adaptive version of a one at time experimentation was used during this
research. Base line testing was completed to understand the individual structural
properties and wave propagations characteristics of the materials. Ballistic testing was
completed to replicate David Fecko's experimental of maximum V_{50} velocity of 947
meter/second and ceramic to composite ratio of 60/40%. Thus enabling future studies to

be completed using data collected from the base line test on to the ballistically tested

materials.

Acknowledgments

I would like to first thank my wife for supporting me through my experience at AFIT. She gave me motivation to continue striving on my thesis during times when it seemed to be the most challenging.

I would like to express my sincere appreciation to Dr. James Blackshire, who took me under his wings to provide guidance and knowledge required to complete my thesis. His insight and experience was certainly appreciated. I am very appreciative of Dr. Som Soni, Roger Wood from Wyle Aerospace Group, and Ryan Reed from ArmorStruxx International for making the logistics of my thesis possible. I also want to thank Dr. Alfred Thal for the academic advisory in the GEM program.

Special thanks to the folks at 46th Test Group for letting me use their ballistic range to conduct ballistic experiments on my thesis.

<div style="text-align: right">Frank T.J. Sha</div>

Table of Contents

List of Figures

List of Tables

STRUCTURAL HEALTH MONITORING OF M1114 HIGH MOBILITY
MULTIPURPOSE WHEELED VEHICLE ARMOR SYSTEM

I. Introduction

With today's wars in Afghanistan and Iraq, it is critical to utilize an all-purpose

vehicle that can maneuver through confined space of downtown Bagdad and Kabul,

nimble enough to climb over steep mountains of Afghanistan, and tough enough to

protect the personnel inside the vehicle. In order to meet the complex requirements, using

a monolithic system of pure steel will not be sufficient because it would become too

heavy and compromise its maneuverability and nimbleness. In order to meet the

requirements of providing light and rapidly deployable vehicles for ground troop, vehicle

engineers are increasingly turning to polymer-matrix composite materials for improved

strength and durability with the addition of minimal weight. Composite materials have

become the main source of lightweight armor for many military vehicle platforms,

including the M1114 Up-Armored High Mobility Multi-Purpose Wheeled Vehicle

(HMMWV). The M1114 Up-Armored HMMWV is the primary vehicle of use by the

U.S. military in Afghanistan and Iraq. While armor technology has been increasing, the

maintenance methods have not been evolving.

The production of the M1114 HMMWVs started in 1996 after the U.S.

government involvement in the Somalia conflict. The military realized insufficient armor

protection was provided on previous generations of HMMWVs. AM General was

awarded the contract to produce a limited number of M1114's with hardened steel armor

with bullet-resistant glass for the passenger cabinet against small arms fire. Even with its

limited protection level of small arms fire, the armor added an additional 2,000 lbs. to the

already heavy weight of 12,100 lb. Still, most of the M1114 produced were of the soft skin variation that did not provide any armor protection. This would prove to be of a major issue when Operation Enduring Freedom (OEF) and Operation Iraqi Freedom (OIF) started.

Since the beginning of Operation Enduring Freedom and Operation Iraqi, the M1114 has been the primary vehicle of use. Due to the fact that a limited number of armored HMMWVs with hardened steel were in place for these two wars, many missions outside of secure bases were conducted with soft skinned M1114 HMMWV. To protect their lives, military personnel using the M1114 HMMWV's decided to take matters into their own hands. Military personnel started to weld on any scrap metal and install ballistic glass that was available in scrap junks. This "hillbilly" armor did provide some level of protection, but it did so while increasing the weight of an already under powered (190 horsepower) vehicle. Besides decreasing the accelerating and braking capability of the HMMWV, it also increased the height of the center of gravity on a vehicle. The higher center of gravity effect is compounded when vehicles are used in mountainous regions of Afghanistan, creating high risk of roll overs.

Due to the ill preparation of logistics prior to the OIF and OEF, Donald Rumsfeld, Secretary of Defense 2001-2006, received heavy public criticism from the public, soldiers, and the parents of the soldiers in Iraq and Afghanistan. During Secretary Rumsfeld's trip to the Middle East, an Army Specialist Thomas Wilson of the Tennessee Army National Guard asked Rumsfeld why his unit's HMMWV's did not have adequate armor:

"We're digging pieces of rusted scrap metal and compromised ballistic glass that's already been shot up, dropped, busted, picking the best out of this scrap to put on our vehicles to take into combat," Wilson said, drawing applause and shouts of approval from his fellow soldiers. "Why do we soldiers have to dig through local landfills for pieces of scrap metal and compromised ballistic glass to up-armor our vehicles?"

Rumsfeld responded that the lack of armor is a "matter of physics," explaining that armored HMMWV's are being produced as fast as they can. "It's a matter of production and capability of doing it," he said.   (Klein, 2004)

Secretary Rumsfeld failed to mention that a $618 million US Senate Bill 1268 "Emergency Supplemental Appropriations Act for Defense, the Global War on Terror, and Tsunami Relief, 2005" was passed in May of 2004 (govtrack.us). It was passed to increase in the production level of the M1114 HMMWV and to increase the armor capability as shown on table 1.

Table 1.1. M1114 Production Capacity

Date	Capacity/Change
May 2003	30 per month
May 2004	US Senate Bill, $618M
Dec 2004	400 per month
Sept 2005	650 per month

Different kinds of armor material have been considered to provide armor protection while decreasing weight of the armor. Aramids (e.g. Kevlar), ultra-high-molecular-weight polyethylene (UHMWPE), and high performance fiberglass (e.g. HJ1) have been the three main composite materials used as armament. The HJ1 composite material has been a popular choice for the M1114 HMMWV. This licensed composite material system complies with the MIL-L-64154 U.S. Military Department of Defense

Specifications and is comprised of high-strength S-2 glass-fiber reinforcements and a phenolic-resin based polymeric matrix. Such armor panels offer superior protection against fragmented ballistic threats compared to monolithic armor panels on an equivalent weight basis (Grujicic, 2006). The HJ1 system with ceramic frontal panels as a two layer system has been used successful as an armor against armor-piercing projectiles (Fecko, 2002).

The HJ1 panel is shown in Figure 1.1 and 2. It has many characteristics that fit as the armament on a M1114 HMMWV, as listed on Table 2. There are some disadvantages in using composite material compared to hardened steel. They are higher cost than steel, complex manufacturing process, complex to repair compared to steel and poor maintenance inspection process.
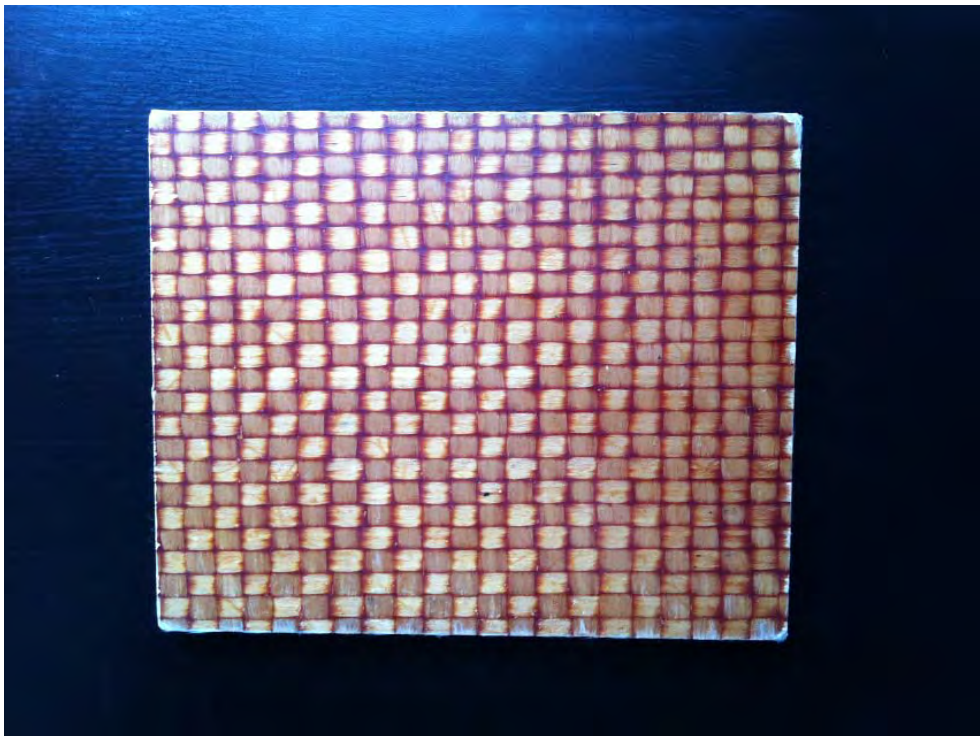
Figure 1.1. Top View of HJ1 Panel
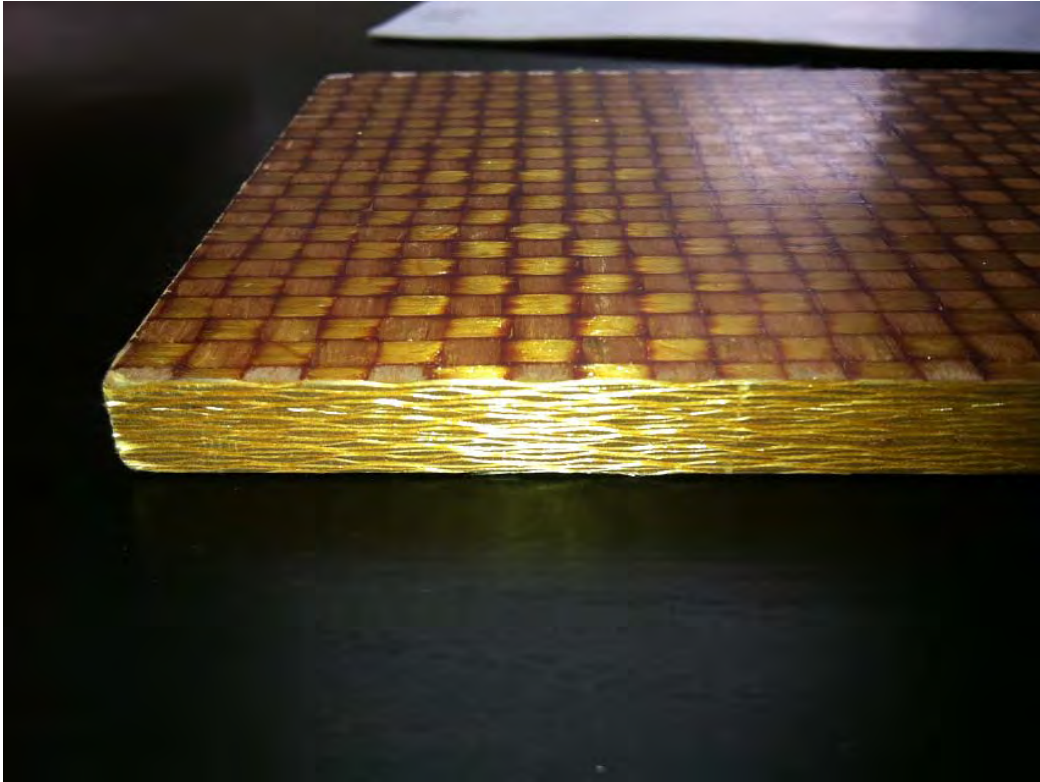
Figure 1.2. Side View of HJ1 Panel

Table 1.2. Favorable Characteristics of HJ1 Panel

Features	Benefits
Higher strength to weight ratio compared to steel	Lighter vehicle, lower center of gravity for handling, increase payload capacity
Fire and flame resistance	Safety
Low smoke and toxicity	Safety
Same ballistic performance as aramid at lower thickness and cost	Low cost of purchase and more space
Low moisture absorption	Remove threat of rust

The most alarming problem with composite armor is the maintenance inspection process of the armor. According to the June 2009 revision of the M1114 Operator's Manual, the procedure method for inspection on the armor components is to "check for armor components for cracks (TM-9-2320-387-10-HR, 2009)." Material failure can occur on a small scale well before there is complete structural failure. Typically matrix/fiber debonding will appear as crazing in neat polymers, with milky appearance where this

localized debonding is occurring. Delamination between plies will result in changes to flexural rigidity, and possible bulking of thickness. Delamination of glass laminates is generally undesirable from a ballistic performance perspective. The bondline between ceramic and composite backing is important. Maintaining structural coupling is necessary for maintaining both single impact and multi-hit performance. Due to the complexity nature of inspecting for structural integrity of composite is there a better non-destructive testing (NDT) detect, locate, and quantify damage on a two layer armor system?

Structural health monitoring (SHM) is the tool that can provide a non-destructive elevation of the structural integrity of the composite armor. SHM is defined as the "acquisition, validation and analysis of technical data to facilitate life-cycle management decisions" (Hall, 1999). SHM denotes a system with the ability to detect and interpret adverse changes in a structure in order to improve reliability and reduce life-cycle costs. The greatest challenge in designing a SHM system is knowing what changes to look for and how to identify them. The characteristics of damage in a particular structure play a key role in defining the architecture of the SHM system. The resulting changes, or damage signature, will dictate the type of sensors that are required, which in turn determines the requirements for the other components in the system. This research project focuses on the relationship between various sensors and their ability to detect changes in a structure's behavior (Kessler, 2001).

In order to establish a structural health monitoring, the following items will be researched:

- What type of sensor is needed?

- Figure out what type of electrical wave signals to detect?

- Identify optimal locations to place the sensors?

- Research what type of system to use a passive system with uncontrolled external input or active system with a controlled external input?

II. Literature Review/Background

HJ1 Composite

Enemy projectile attacks received by the M11114 HMMVW's are usually small arms fire. Small arms ammunitions fall into two categories, non-armor piercing (AP) and armor piercing (blunt) projectiles. The S-2 glass phenolic HJ1 composite armor system has been one of the primary methods of up-armament of the HMMWV. It is a patented system created by AGY, located in Aiken, South Carolina.

HJ1 is based on AGY's S-2 glass reinforcement of woven roving fabric and a phenolic resin that is laminated into hard armor panels. The S-2 glass HJ1 was developed in the late 1980's and been extensively researched for the past two decades (Hartman, 1986). It has been used in multiple military platforms. S-2 glass fiber reinforced laminates is critical to ballistic performance due to its high tensile and compressive strengths. The combination of materials results in a composite that has superior ballistic protection, excellent durability, and outstanding fire, smoke, and toxicity resistance. The system has been tailored for producing large flat panels using a compression molding process. Overall economics are attractive in that a 25 to 40 percent cost savings over comparable performing aramid armor systems is provided. The fiber has a high ultimate elongation of 5.7% which is vital to its impact-absorbing characteristics. The HJ1 meets the military regulation requirements by the Army for "intended for use as a component of composite armor (MIL-DTL-64154B)." HJ1 has been proven to be effective against non-armor piercing (AP) projectiles, but not against AP projectiles.

Non-AP/AP Projectile Testing

When a blunt projectile contacts a hard surface, it is decelerated significantly by the initial intense impact shock wave. Furthermore, blunt projectiles are less effective at penetrating the armor because they have to cut the encountered fibers in two places and to accelerate the material in front of the projectile in the rearward direction (Grujicic, 2006). On the other hand, metal armor laminated with composite is insufficient against armor piercing projectiles. An AP projectile is typically comprised of a sharp, hardened steel or tungsten carbide penetrator covered with a guiding metal jacket that adds mass and allows the projectile to conform to a rifled barrel to produce spin for accuracy. The sharp tips of armor piercing projectiles are able to push the fibers away in the lateral directions, causing the fibers around the penetration cavities to buckle (Grujicic, 2006). Fiber buckling, a localized deformation process, is generally associated with little energy absorption. This explains why armor-piercing projectiles are so effective against all fiber-reinforced polymer-matrix composite armor like HJ1. Neither the fibers nor the matrix of the composite material are hard enough to cause blunting of the AP projectile's sharp, hardened penetrator nose. To counteract the penetrating characteristics of an AP projectile, HJ1 composite is used in conjunction with Al2O3 ceramic tiles as a frontal plate.

Alumina (Al$_2$O$_3$) Ceramic Frontal Plate

Alumina (Al$_2$O$_3$), used in the form of ceramic tiles, is light, hard, and strong in compression. Figure 2.1 is an example of a alumina ceramic frontal plate. When a ceramic tile sustains a ballistic impact, the face of the tile experiences compressive forces, against which ceramics are extremely strong and typically will not fail. Erosion of

the projectile tip occurs first, followed by failure of the ceramic in tension as the compressive shock wave reaches the back surface of the tile and is reflected as a tensile wave (Langford, 1989). However, by the time the ceramic fails, it has absorbed some energy, but more importantly it has eroded the tip of the projectile so that it cannot easily push aside the fibers in the composite backing. This is illustrated on Figure 2.2.

Figure 2.1. Ceramic Frontal Plate
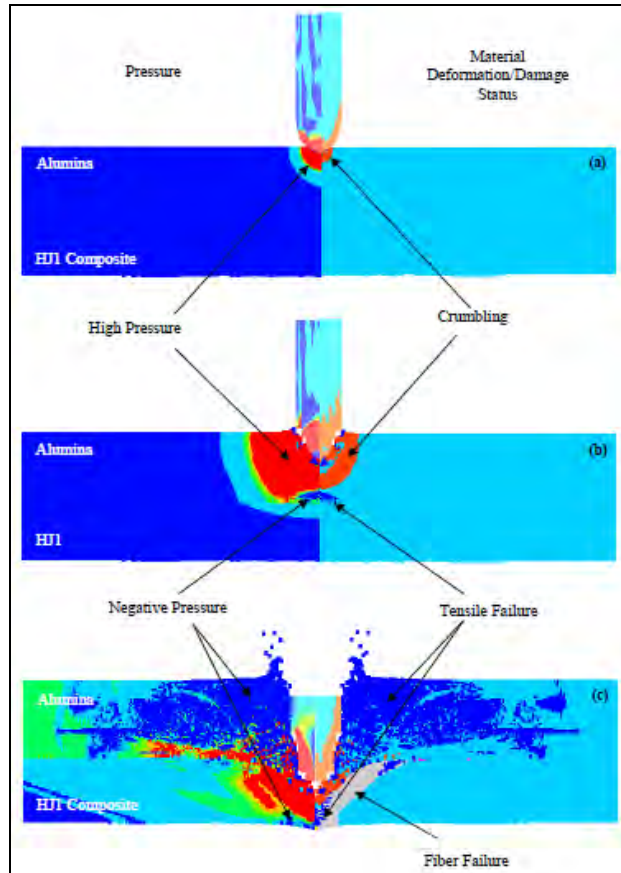
Figure 2.2. The left side illustrates the evolutions of pressure and material deformation/damage status on the right on the two layer armor (Grujicic, 2006)

The composite backing material (HJ1) serves a dual purpose; it carries the bulk of the load when the armor is used for structural applications in addition to ballistic protection. It also absorbs the kinetic energy of the armor-piercing projectile once its tip is blunted. The kinetic energy is absorbed through a combination of fiber strain and fracture, fiber pullout, and composite delamination. Figure 2.3. illustrates a coupling of the ceramic and composite as an armor system.

Figure 2.3. Two Layer Armor with Ceramic Frontal Plate and HJ1 Composite

Ballistic Testing

Studies have been conducted to calculate the optimal ratio of composite backing to ceramic facing areal densities at a fixed overall areal density, because it is an important design parameter in hybrid armor. Ballistic tests have been conducted to measure performance of several HJ1-based hybrid armor panels hard-faced with Al2O3 ceramic tiles, all with a fixed total areal density of 51kg/m2 against the .30 caliber M2 AP projectile (Fecko, 2002). The experimentation proved that 40% is the optimal HJ1-composite content (defined as the percent of total areal density allotted to the HJ1 for the hybrid armor to be maximized with a maximum velocity of 948 meters/second. The optimal ratio has been established, but the HJ1 system with ceramic frontal plate can still fail. But how would an inspector know if it has failed and the most inner layer of the system, the S2 glass, has been compromised? If a non-AP or AP projectile did not penetrate the HJ1 armor, it would be difficult to identify damage to the S2 glass, especially at the microscopic level. A structural health monitoring (SHM) system can be the non-destructive evaluation tool that can be used to detect and determine property changes that are not within the operational specs.

Structural Health Monitoring

SHM has been around since the beginning of 19th century when railroad wheel-tappers have used the sound of a hammer striking the train wheel to evaluate if damage was present. In rotating machinery, vibration monitoring has been used for decades as a performance evaluation technique (Dawson, 1976). Today's advance automobiles have SHM indicators of the engine performance available to the vehicle operator. The check engine light of the vehicle will light up when there is an engine problem, alerting the operator to have the vehicle inspected by a mechanic. The mechanic will connect a code scanner to the automobile's computer that will provide an error code for the problem. The code can indicate if there is knocking between the piston and cylinder walls due to engine predetonation, incorrect air to fuel mixture measured by the oxygen sensors on emission components, misaligned on the valvetran assembly scanned by the timing sensors and etc. SHM has been used for many structural applications for detect and predict damage.

With China's infrastructure growing to support their massive industrial and economic growth, constructing long-span bridges have been a priority for their national transportation system. Utilizing SHM on these bridges has become critical to maintaining situational awareness of the structural integrity of the bridges. SHM enables China's Transportation Agency to manage over a hundred long-span bridges placed crossed the second largest country in the world. Sensors are placed a crossed the bridge collecting temperature, wind, vehicle load, and pier settlement data as input, see Figure 2.4. The output data that would be critical to get a structural prognosis of the bridge are mid-span deflection, cable force, displacement, and strain. The monitoring of mid-span deflection

of main beam is the critical part in bridge health monitoring system since it is the key

indicator to the overall performance of the bridge (Li & Sun, 2011).
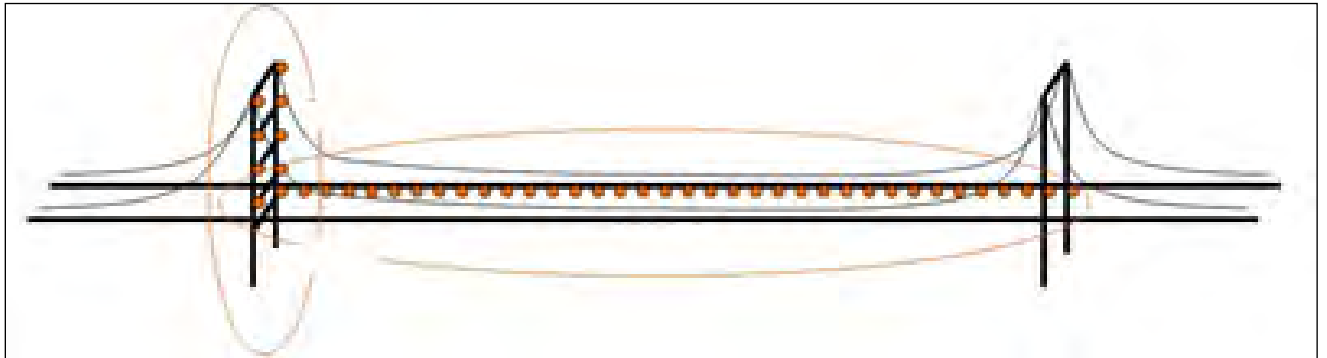
Figure 2.4. Example of a Bridge with Sensors Placed (Kim, Pakzad, Culler, Demmel, Fenves, Glaser & Turon, 2007)

Lamb Waves

Lamb waves were first described by a mathematician named Horace Lamb in 1917

as a form of elastic perturbation that can propagate in a solid plate with free boundaries

(Viktorov, 1967). The particle motion is on the plane that contains the direction of the

wave propagation and perpendicular to the plate. Elastic waves in solid materials are

guided by the physical boundaries of the plate that it propagates on. The propagation of a

Lamb wave in a material can be described with the dispersion curve, which plots the

phase and group velocity versus the excitation frequency (Kessler, Spearing & Soutis,

2002). Lamb waves propagate on the surface boundaries. This creates large amout of

attenuation that could be difficult to understand and analyze.

Bulk Waves

Bulk waves are identified as wave propagation through a material parrallel to the

contact surface.

Transverse Waves

Transverse waves are waves that are moving perpendicular to the direction of propagation. If you anchor one end of a ribbon or string and hold the other end in your hand, you can create transverse waves by moving your hand up and down. Notice though, that you can also launch waves by moving your hand side-to-side. This is an important point. There are two independent directions in which wave motion can occur (Russell, 1999).

Longitudinal Waves

Longitudinal waves, are waves that have the same direction of vibration as their direction of travel, which means that the movement of the medium is in the same direction as or the opposite direction to the motion of the wave. Mechanical longitudinal waves have been also referred to as compressional waves or compression waves (Russell, 1999).

Pulse Echo

Pulse echo method uses the transducer to perform both the sending and the receiving of the pulsed waves as the wave is reflected back to the device. Reflected ultrasound comes from an interface, such as the back wall of the object or from a structural change within the object. The oscilliscope (Nondestructive Testing Handbook).

Pitch Catch

The pitch catch method uses one transducer to send a ultrasound wave through one surface, and a separate receiver detects the amount that has reached it on another surface after traveling through the medium. Imperfections or other conditions in the space

between the transmitter and receiver reduce the amount of sound transmitted, thus

revealing their presence (Nondestructive Testing Handbook).

Piezoelectric (PZT) Sensors

Lead zirconante titanate also referred to as PZT, these sensors are used to induce and

receive ultrasonic Lamb waves, see Figure 2.5. PZT materials exhibit an effect whereby

they expend or contract in the presence of an applied electrical field (Gautschi, 2002).

The electrical source can be a waveform generator like the one on Figure 2.6. The

propagated waves received by the PZT sensor will be outputted to the oscilloscope to

collect data, see Figure 2.7.

Figure 2.5. PZT Sensor used to Induce and Collect Wave Propagation

Figure 2.6. Waveform Generator

Figure 2.7. Oscilloscope

The velocity of the wave produced by a piezoelectric sensor induced at a frequency can easily be verified in a control (undamaged) specimen by measuring the time-of-flight (TOF) in an oscilloscope between two sensors of known separation. This information can then be used to locate damaged areas along a specimen, without using any analytical models, by observing the change of wave propagation characteristics between the sensor and actuator.

The velocity of the waves varies to the resonance frequency of the structure it propagates on, so if the stiffness of the structure has been reduced, the velocity will reduce. The other indicator of damage is reflection of waves once it is contacts the new boundaries created by the damage, creating a decrease in magnitude of wave propagation receival. From these two pieces of information, correlation can be determined to identify damage location and magnitude.

Tomographic Reconstruction

In tomographic reconstruction, an array of PZT sensors is mounted around the area of interest as shown in Figure 2.8. Wave signals are sent and received from each PZT sensor using a pitch-catch method. Signal features are selected and analyzed to create a computed tomographic image (Lissenden & Rose, 2008). The reconstruction algorithm accounts for wave scattering and reflections from damage using a probabilistic method that results in the final tomography being a superposition of ray ellipses sees Figure 2.8.
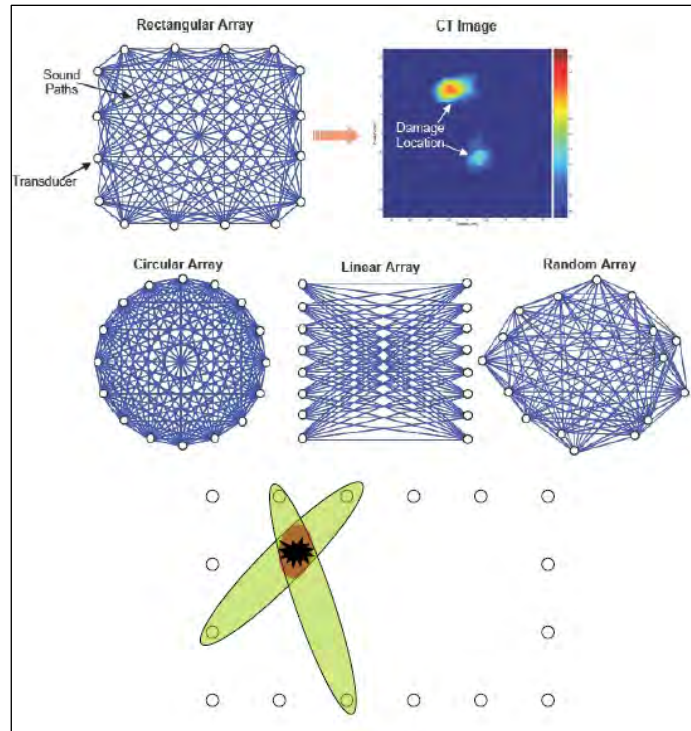
Figure 2.8. Diagram of PZT Sensors Showing Chords between Sensors and a Computed Tomographic Image of Damage on Sample Plate (Lissenden & Rose, 2008)

Computed tomographic reconstruction has been used in many industries. Since the 1970s, computed tomographic reconstruction has become a crucial tool in the medical industry. Tomographic reconstructions has been used for medical imaging of human internal organs and bone structures using conventional x-ray tomography, where the X-ray technician captures images of the body by moving an X-ray source and film in opposite directions during the exposure. Three-dimensional images are created by taking images around a single axis of rotation, see Figure 2.9.

Figure 2.9. X-Ray Images Taken Around a Single Axis Rotation to Create a Three-Dimensional Image (Donaldson, 2010)

Specific uses of ultrasonic Lamb waves on tomographic reconstruction have been used to monitor the structural integrity of pipelines. On Figure 2.10, PZT sensors are placed to form two vertical arrays around the circumference of a 10" steel pipe (schedule 40) at two different axial positions 48" apart (Royer, Velsor & Rose, 2009). Ultrasonic waves are induced and acquired between the two boundaries using all possible combinations of pitch-catch patterns between inducing and receiving sensor. Preliminary data sets were collected as a baseline data set for an undamaged pipe. Material was removed to form damage and new data sets were collected from the PZT sensors. A tomographic image was reconstructed by comparing the undamaged and damaged data, see Figure 2.11.

Figure 2.10. Photo Showing One Setup for Using CT Approach for Pipeline Health Monitoring (Royer, Velsor & Rose, 2009)
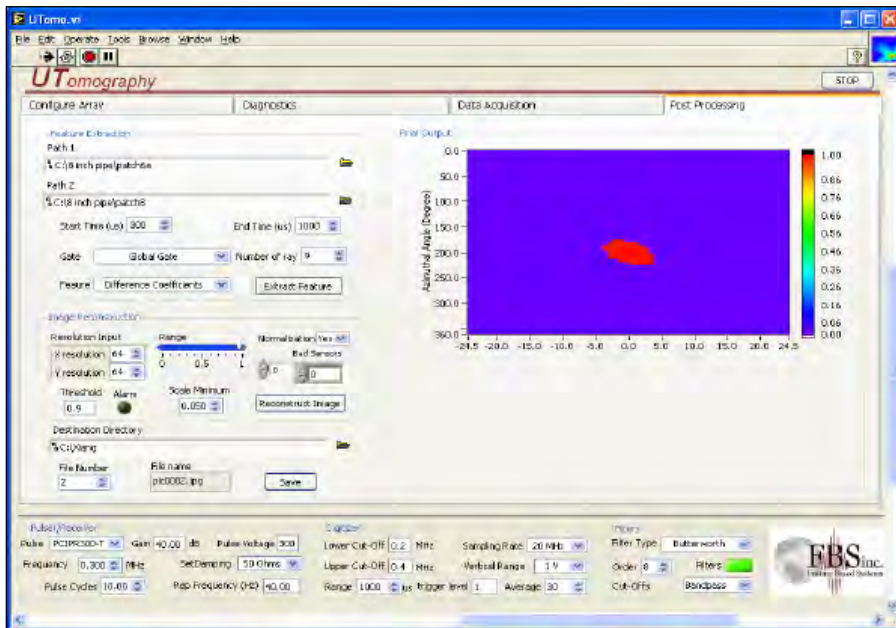
Figure 2.11. CT Image for the 10" Pipeline with Damage (Royer, Velsor & Rose, 2009)

Once the scan data has been acquired, the data must be processed using a form of tomographic reconstruction, which produces a series of cross-sectional images. There are two techniques, parallel projection tomography and double-crosshole.

Parallel Projection Tomography

The simplest technique is parallel-projection tomography, where transducers are scanned along parallel lines using PZT sensors to induce and receive ultrasonic wave propagations. At each position, time of arrival and amplitude are measured and recorded. Once the pitch-catch measurements for each orientation are collected, the pitch-catch arrangement rotates at a fixed amount and data is measured and collected again until. An example array consisting of seven parallel sensors (pitch catch) for four orientations (0◦, 45◦, 90◦ and 135◦) are shown in Figure 2.12. In actual practice, the more PZT sensors used on the setup and smaller increments of angular rotations are used, the more detailed the tomographic reconstruction will be. The method to rotate the array is to it rotate the sample or to rotate the sensor assembly. Both are not practical in the field condition (Leonard, Malyarenko & Hinders, 2002).

Figure 2.12. Parrallel Projection Tomograpghy (Leonard, Malyarenko & Hinders, 2002)

Double-Crosshole Tomography

    An alternative to parallel projection technique is the double-crosshole technique.

This technique uses the geometries and algorithms developed from the seismology field

to record a criss-cross ray pattern. Two arrays can be set up, but to increase ray density

for increased data resolution, four arrays should be used to create a box setup. The

double-cross technique uses the simultaneous iterative reconstruction technique to solve

the inverse problem of recovering an object from its projections. This technique takes

advantage of ultrasonic wave's flexibility and iterative nature. This allows for any

scanning geometry and still be used with incomplete data sets. Traditional parallel

projection algorithm requires predetermined scanning configurations, complete data set

without errors, and absence of noise. Figure 2.13 illustrates the geometry of the double-

crosshole setup, where the circles on the perimeter are the individual PZT sensors. The

23

pitch-catch ultrasonic wave propagations are collected using every possible combination along the i and j axis. The individual wave propagation is digitally recorded and compiled to create a tomographic reconstruction model of the structure (Leonard, Malyarenko & Hinders, 2002).
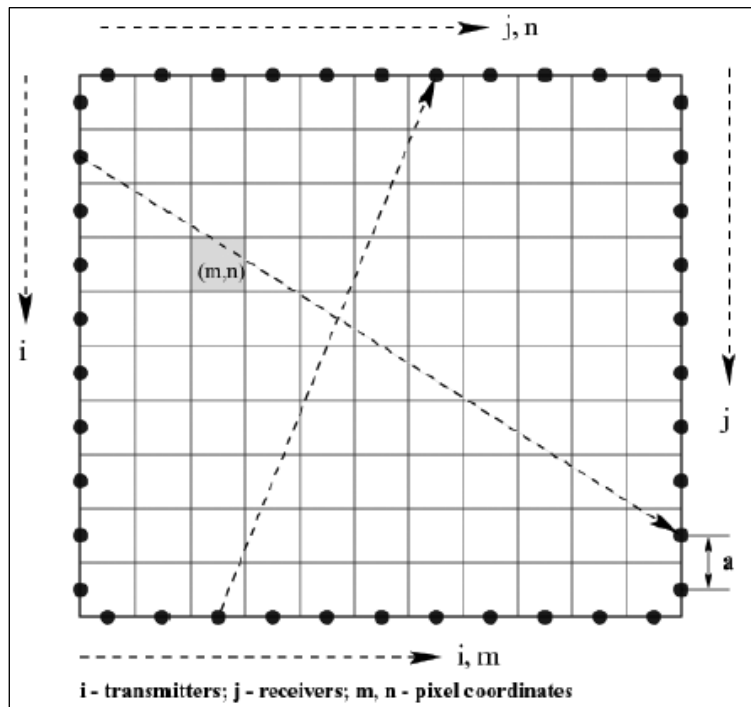
Figure 2.13. Double-Crosshole Tomography (Leonard, Malyarenko & Hinders, 2002)

Past Passive Structural Health Monitoring Experiment

In an experiment conducted by facility of University of Purdue in conjunction with the US Army Research Laboratory, vibration-based structural health monitoring was successfully conducted on one layer S-2 composite system, see Figure 2.14. The researchers were successfully able to passively identify the external force, identify the amount of damage, and quantify damage (Stities, 2007). Damaging impact energy (weighted hammer test) was applied to the test specimens and the passively measured frequency response of the armor was used to produce a dynamic model of the specimen

and the subsequently estimate calculate the level of damage on the specimen (Brush, D.E., Zwink, & Walsh, 2009).

Figure 2.14. Passive Structural Health Monitoring on S-2 Composite Armor

The researchers were able to correctly identify the location of the impact 93.4% of the time, while 100% identification was produced within a 1" of the actual impact location. Impact identification was done using a single tri-axial accelerometer to calculate the force impact. The major limiting factor of this research is that the impact was completed by dropping 4.5, 5.25, and 6.0 lb. weights on to the S-2 composite. This produced a small amount of damage compared to a .30 AP projectile. It is also limited to single layer sensing instead of two layers.

Past Active Structural Health Monitoring Experiment

This experiment, Figure 2.15, was conducted for damage detection of composite structures by developing an improved wavelet based signal processing technique that enhances the visibility and interpretation of the Lamb wave signals related to defects in a composite plate (Sohn, Park, Wait, Limback, & Farrar, 2003). In addition, a statistically rigorous damage classifier is developed to identify wave propagation paths affected by damage. Finally, a new damage location algorithm is proposed to locate damage based on signal attenuation rather than time-of-arrival information. PZT sensors were used to

capture the wave signals. Actuators were used in conjunction with the PZT sensors to

produce the Lamb waves. Thus wave inputs were actively produced for analysis. The

material itself was very thin. Lamb waves were used instead of bulk waves. The

experiment was only conducted on a single layer platform, not a two layer platform.
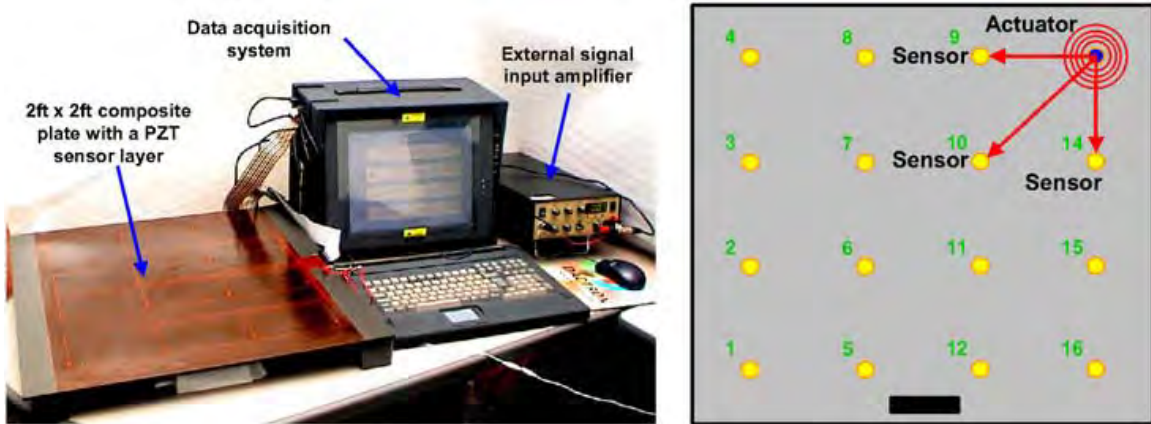

Figure 2.15, Active SHM

III. Methodology

Experimental Plan and Goals

The overarching style of the experiment is an adaptive version of one-at-a-time (Ion, 2004) experiment following Middendorf's division of experimentation: device evolution, repeated analysis, and synthesis (Middendorf, 1986). The first portion of the experiment is to exam the individual components of the two layers composite armor individually and the two together as a system. The base line data would be used to understand wave propagation characteristics of the materials individually and together. Experiments will be conducted with and without controlled damage. The base line tests can provide information on either it is possible to conduct SHM evaluation using bulk waves and if it is possible to evaluate two layers of material with only one set of sensors. Ballistic testing will conducted replicating David Fecko's experiment on maximum velocity of project impact and composition ratio of ceramic to composite. Lastly, applying SHM evaluation techniques understood from the base line testing to conduct SHM evaluation on the ballistically tested panel.

Hypothesis

H_1 = NDE through SHM is possible by detecting, locating and quantifying amount of damage on a two layer armor system

H_0 = NDE through SHM is not possible on a two layer armor system

Base Line Testing

Conducting the base line experiments on test coupons of the individual components of the armor was critical. It enabled base line data collection and examination of the materials in a manageable level. Conducting the base line testing with

27

the small coupons made it manageable. The actual purchased panels fabricated by ArmorStruxx were large and very heavy, which would have created complication during base line testing. More importantly, the purchased panels were expensive and required a six week turnaround time once placed on order. Free test coupons of the ceramic and HJ1 composite were provided by ArmorStruxx.

Scope and Limitation

The intent of the base line portion of experimentation was to understand the physical characteristics of the material individually and together with and without controlled damage. By conducting base line testing in a laboratory where data can be collected during each step of procedure, it allowed for a controlled and logical understanding of the wave propagation characteristics of the two different materials. This controlled base line portion of the experiment was critical to understanding and simulating the physical changes after the two layer armor system that would have been damaged. The base line portion was to examine how the materials responded to different wave frequencies. Figure 3.1, demonstrates the overall layout of the experimental set up. Bursts of wave propagation are produced from the wave form generator and used as the input wave through the ceramic and composite. The wave propagation output through the ceramic and composite is captured and displayed on the oscilloscope.
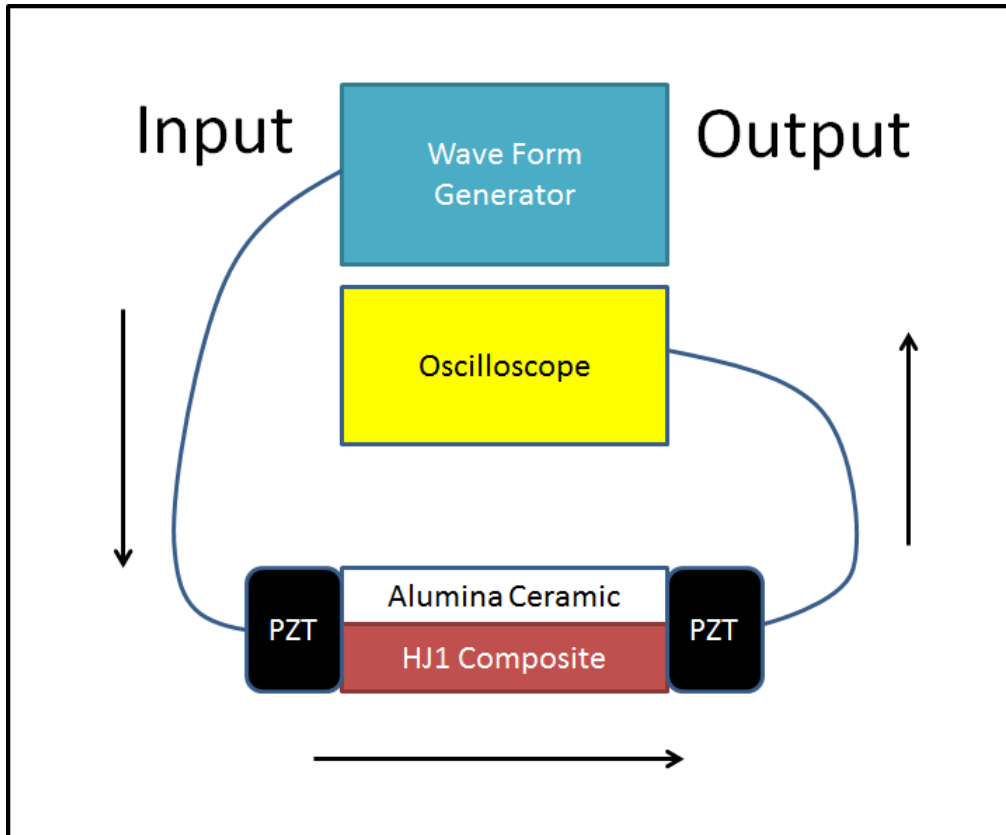
Figure 3.1. Base Line Experimental Setup

Constraints and Boundaries

The availability of equipments was limited to those available in the AFRL/NDE laboratories. The type of sensors was a limit. Having only two sensors created a major constraint by having to repeat the same measurement numerous times at different locations, instead of making one pass of a set frequency with multiple sensors at different locations. The data was recorded on to the floppy drive of the oscilloscope. This was also limitation due to the limited amount of 1.44 MB data storage capacity of the drive. This required for the data on the floppy drive to be transferred over to a larger storage device, which became very time consuming as the storage limit will be reached after only six passes of wave propagation. Only pitch-catch of wave propagation data was collection. This is due to the fact that pulse echo did not work. There was no signal capture back

29

from the bounce from the structural boundary of the coupons. This would be due to the fact that the wave energy would have been dissipated throughout the structure of the composite thus eliminating any measure signal at the end. This reflects the energy absorption property of the composite designed to spread impact load.

Equipment

- HJ1 Composite test coupon, Figure 3.2

Figure 3.2. HJ1 Composite from ArmorStruxx

- Five Ceramic test coupons, Figure 3.3
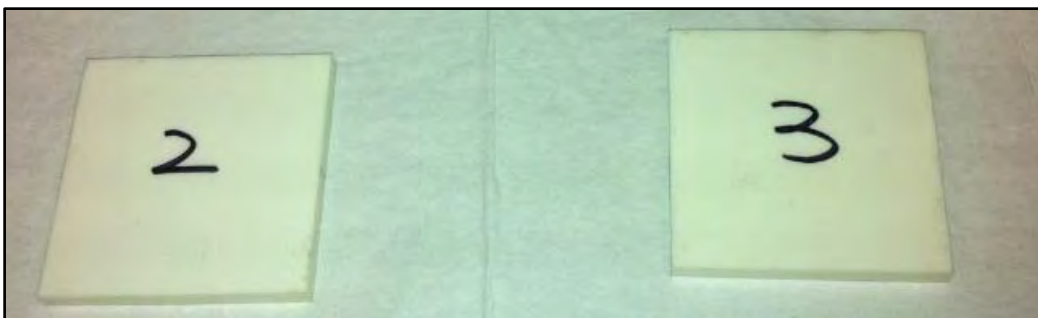
Figure 3.3. Ceramic Coupons 2 and 3 (Total of 5)

- Agilent 80 MHz Function/Waveform Generator, Figure 3.4

  o Model: 33250A

  o Calibrated 14 April 2010 Figure 3.5

Figure 3.4. Agilent 80 MHz Function/Waveform Generator, Model 33250A
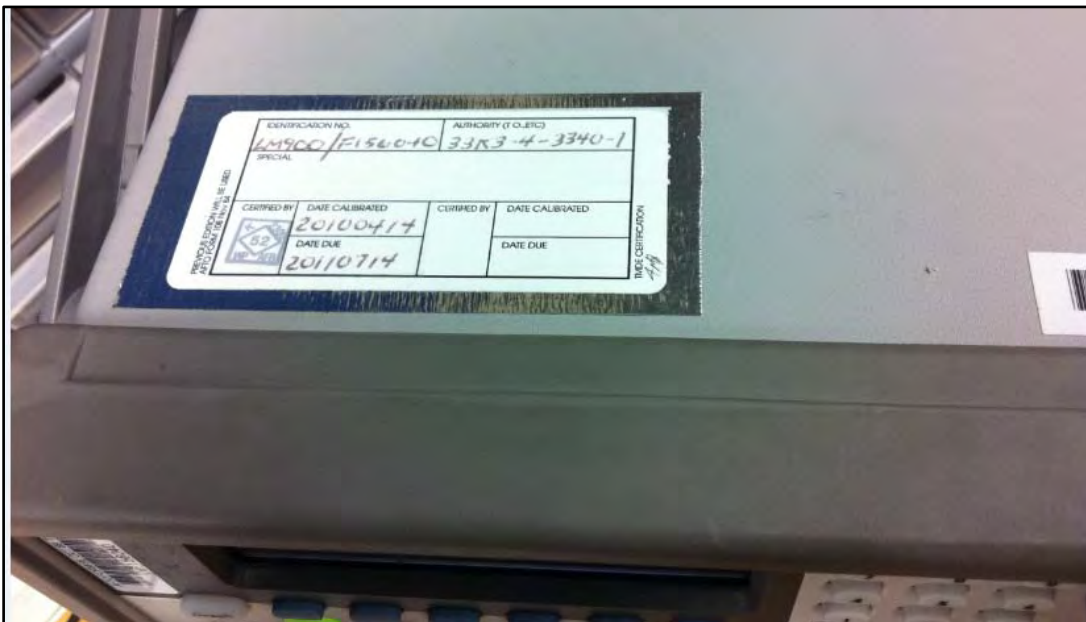
Figure 3.5. Calibration Sticker of the Digital Oscilloscope

- LeCroy Digital Oscilloscope, Figure 3.6

o   Model LT584

o   Calibrated: 21 October 2010, Figure 3.7

Figure 3.6. LeRoy Digital Oscilloscope, Model LT584

Figure 3.7. Calibration Sticker of the Digital Oscilloscope

- Mitutoyo Digital Caliper, Figure 3.8

    o Model: 500-352

    o Calibrated: 14 December 2010 Figure 3.9

Figure 3.8. Mitutoyo Digital Caliper
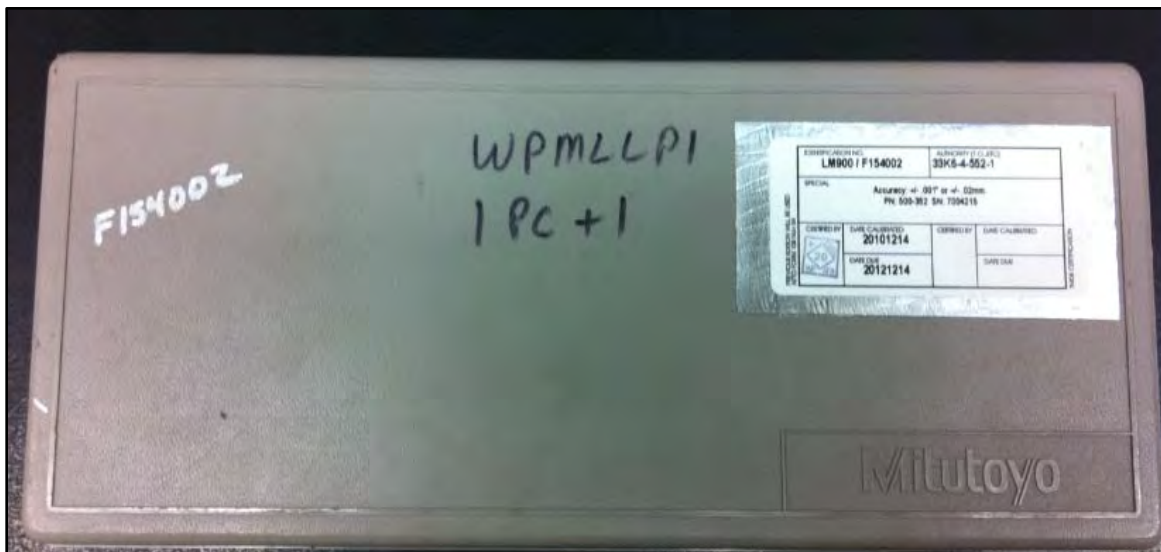
Figure 3.9. Calibration Sticker of the Mitutoyo Digital Caliper

- Two Piezoelectric Longitudinal Wave Sensors, Figure 3.10

    o 1 MHz capacity, 0.5" diameter

    o Calibrated: 28 Jun 2011

Figure 3.10. PZT Sensors

- Four Irwin's 6" Quick-Grip, Figure 3.11

  o Model: 546HD

Figure 3.11. Irwin Quick-Grip Clamps

- Jet JTM-1050 Mill/Acu-Rite, Figure 3.12

    o Model: 6-200-010

Figure 3.12. Jet JTM-1050 Mill

- Starlite Diamond Grinding Bit, Figure 3.13 and 3.14

    o Model: 115060

    o Diameter: 0.14"

    o Grit Size: 140
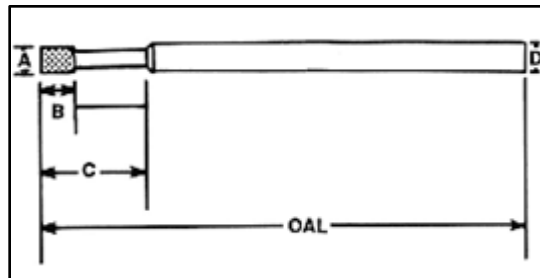
Figure 3.13. Starlite Bit

Figure 3.14. Starlite Bit Casing with Product Information

- Generic Vacuum Coupling Grease

- Precision rotating saw

- Mounting structure to hold the coupons in place, Figure 3.15
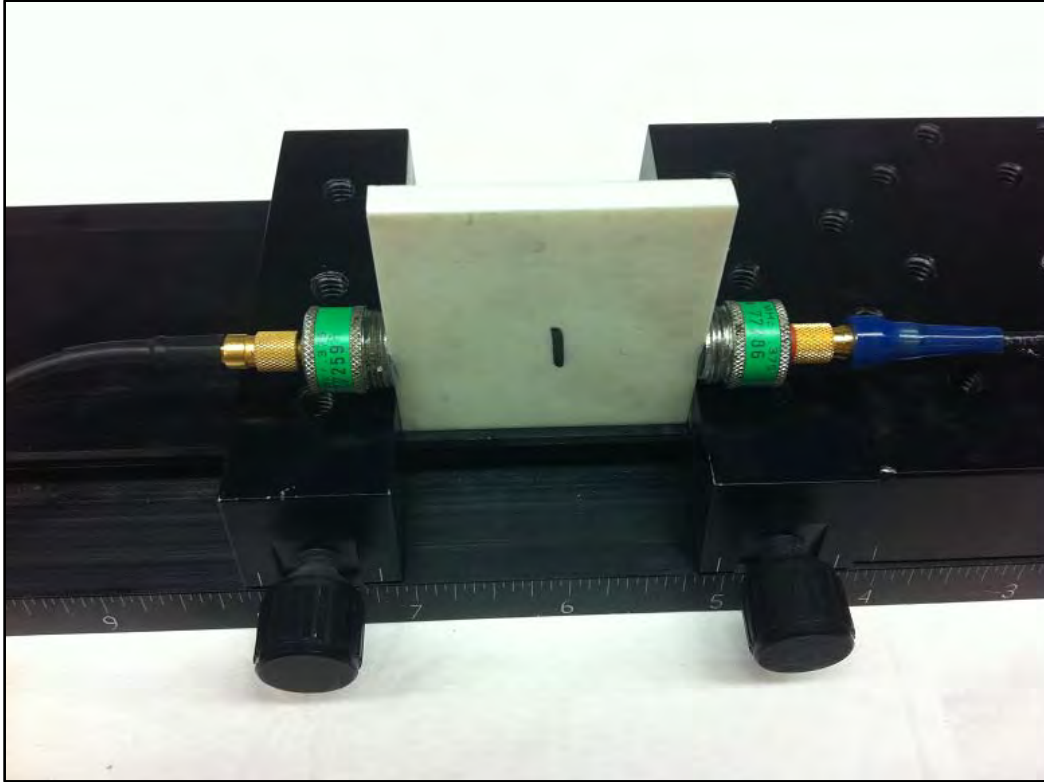
Figure 3.15. The Mounting Structure Holding Ceramic Coupon

Validity

Internal validity of the experiment is demonstrated by using cause and effect throughout the experiment. The experimental procedures were adjusted from trial and error. Replicability of the experiment was completed by using same frequency settings and sensor locations on each of the test coupons.

Independent Variables

- Location of PZT sensors

- Wave frequency (300 KHz to 1000 KHz)

- Tone burst cycles (1 or 5)

- Input voltage

- Controlled depth and diameter of damage on the ceramic panel

Dependent Variables

- Type of wave propagation

- Time of flight of wave propagation

- Output voltage of wave propagation

Procedure

1) The first step was to measure the dimensions of the five ceramic coupons, see

Figure 3.16.

Figure 3.16. Measuring the Dimensions of Ceramic Coupon #3

2) Use a precision rotating saw to cut a 50 mm X 50 mm piece of test coupon from the original HJ1 composite sample (139.0142 mm X 113.8301 mm). This will match the ceramic's dimensions.

3) Cut other HJ1 coupons of varies sizes, see Figure 3.17.

Figure 3.17. Various Different Cuts HJ1 Coupons

4) Measure and record the dimensions of the HJ1 coupons

Table 3.1. Dimensions of the Various HJ1 Coupons

		Measurement #1	Measurement #2	Measurement #3	Average
Composite #1	Height	1.9915	1.993	1.993	1.9925
	Width	0.05	0.0525	0.05	0.050833
	Thickness	0.4515	0.4505	0.4505	0.450833
Composite #2	Height	1.958	1.963	1.964	1.961667
	Width	0.446	0.446	0.48	0.457333
	Thickness	0.461	0.461	0.46	0.460667
Composite #3	Height	1.942	1.94	1.9415	1.941167
	Width	1.5235	1.5245	1.5275	1.525167
	Thickness	0.442	0.4425	0.442	0.442167
Composite #4	Height	1.992	1.9935	1.9935	1.993
	Width	0.449	0.4495	0.449	0.449167
	Thickness	1.984	1.985	1.985	1.984667
Composite #5	Height	2.529	2.5265	2.5265	2.527333
	Upper Width	1.991	1.991	1.991	1.991
	Lower Width	1.423	1.4215	1.423	1.4225
	Thickness	0.4455	0.4455	0.4455	0.4455

5) Conduct wave propagation experiments on composite samples 1 through 5 to determine optimal frequency settings for the rest of the experiment, see Figure 3.18 and Figure 3.19.

    I.   Place the composite on the secured mounting platform.

    II.   Place a PZT sensor on each side of the composite with a small amount of coupling grease.

    III.   Ensure that the PZT sensors are placed in a straight line to optimize capturing of the wave propagation data.

    IV.   Use the Irwin Quick-Grip to secure the sensors in place.

Figure 3.18. Top View of the Composite Coupon on the Mounting Platform with PZT Sensors Clamped on to the Coupon

Figure 3.19 Another top View of the Composite Coupon on the Mounting Platform with PZT Sensors Clamped on to the Coupon

V.   Settings on the wave form generator see Figure 3.20.

VI.   300-1000 KHz (100 KHz intervals).

VII.   Tone bursts of 1 and 5 cycles.

VIII.   Period (2 – 5 µs, which ever that presented a clean output).

Figure 3.20. Waveform Generator Used to Create Input Wave Propagations

IX.   Record data on the oscilloscope, Figure 3.21.

X.   Record max pike-to-pike voltage (mV) on the floppy drive.

Figure 3.21. Oscilloscope Used to Capture Output Wave Propagations

6) Repeat step 5 for the five ceramic coupons, see Figure 3.22.
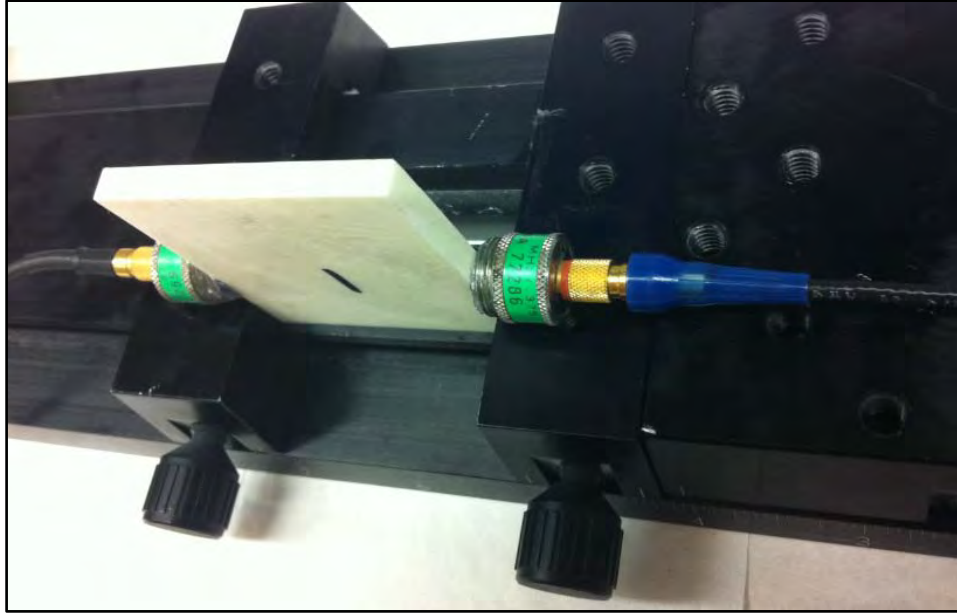
Figure 3.22, Ceramic Coupon #1 on the Mounting Platform with PZT Sensors Clamped

7) Repeat step 6 and collect data with the composite (sample 4) and ceramic

(sample 4) clamped together; see Figure 3.23 and Figure 3.24.
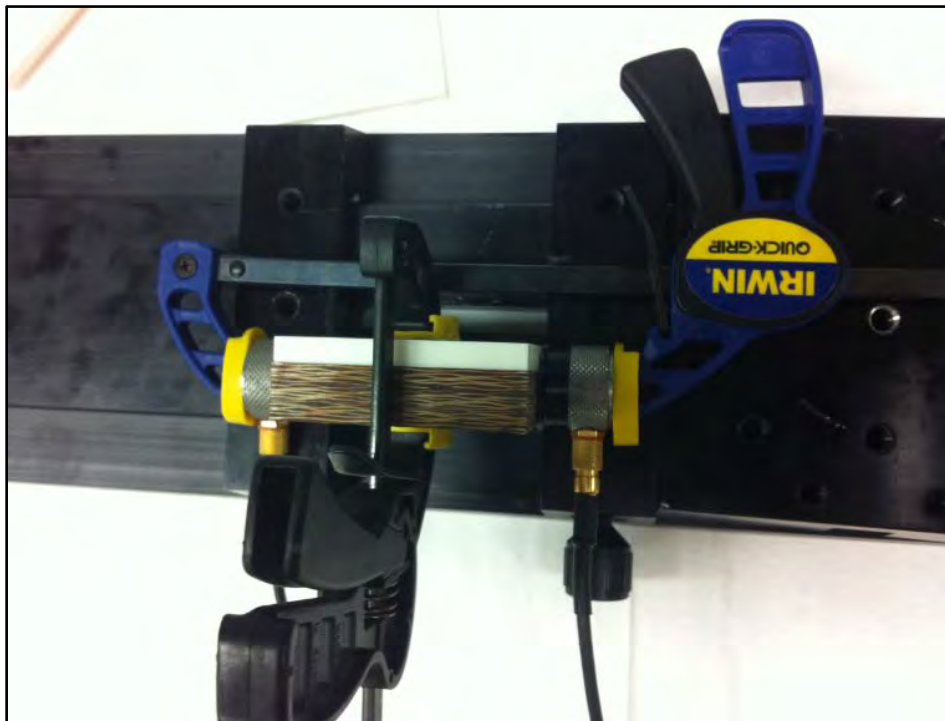
Figure 3.23. Top View of the Composite and Ceramic Coupons on the Mounting
Platform with PZT Sensors Clamped
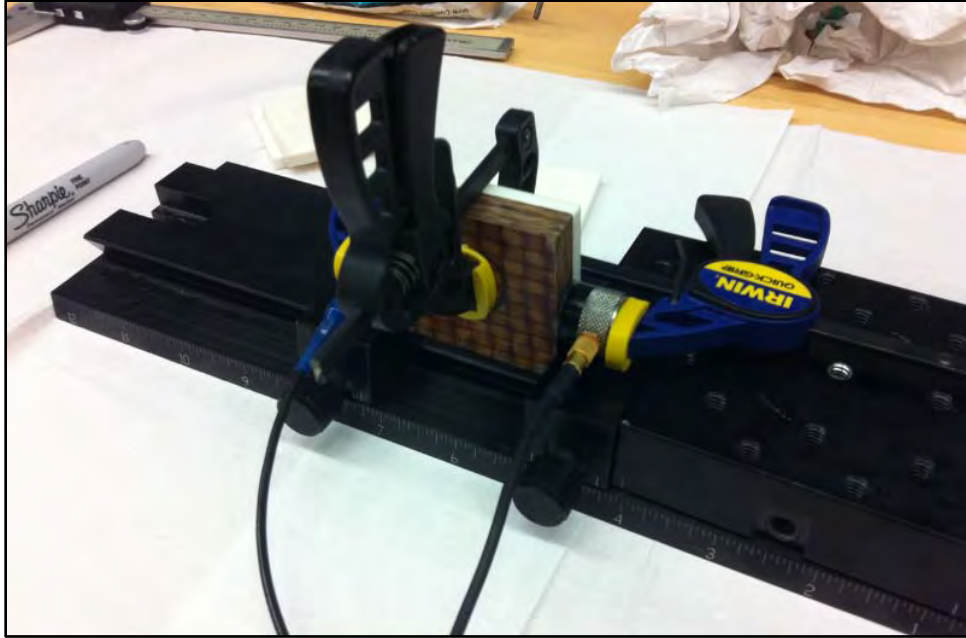
Figure 3.24. Another Top View of the Composite and Ceramic Coupons on the Mounting Platform with PZT Sensors Clamped On

8) Repeat step 7 without the ceramic, but with the sensors in the exact location as if the ceramic was still present. See Figure 3.25.
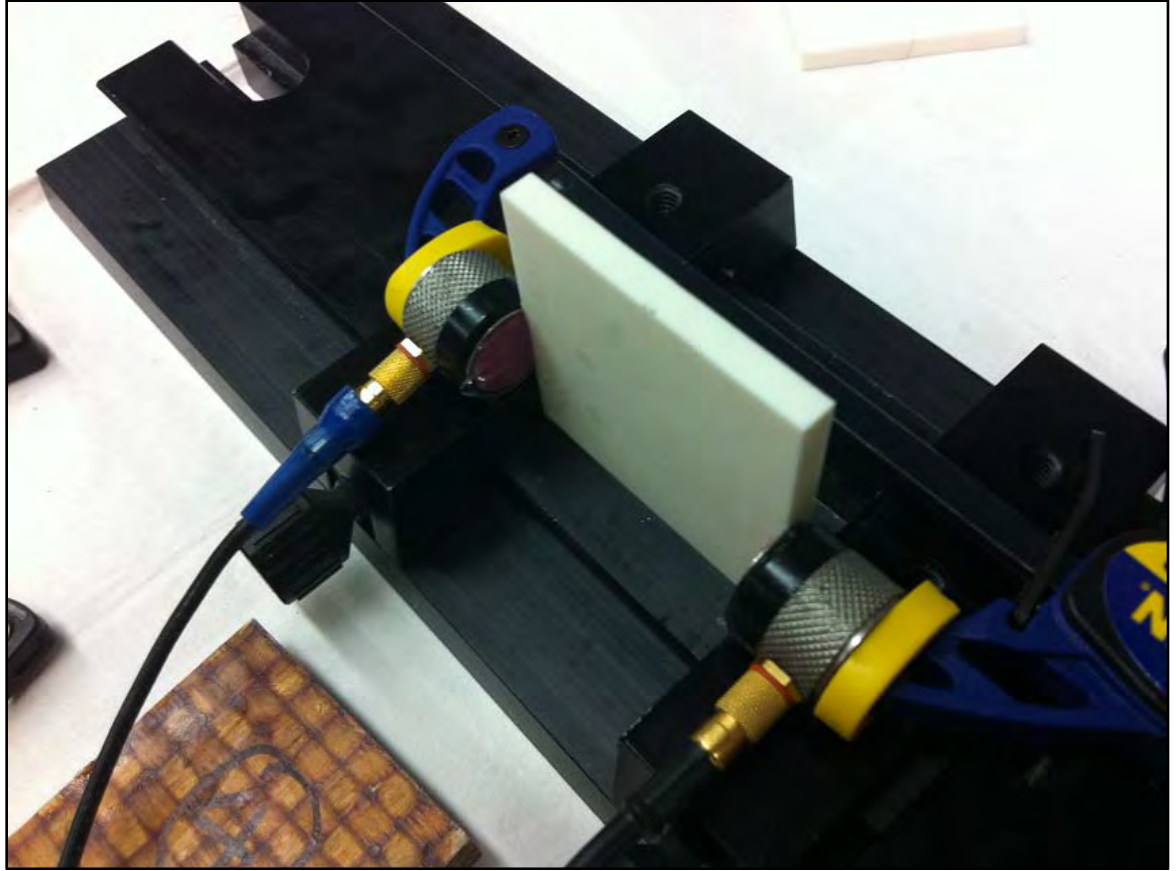
Figure 3.25. PZT Sensors Placed on the Ceramic in an Offset Orientation

9) Repeat step 7 without the composite, but with the sensors in the exact location as if the composite was still present. See Figure 3.26.

Figure 3.26. PZT Sensors Placed on the Composite in an Offset Orientation

10) Analysis the data sets of the composites and coupons on amplitude versus time plots to determine optimal frequency input for the rest of the experiment.

11) Divide each sides of the composite into four sectors, see Figure 3.27.

Figure 3.27. Composite #4 with the Divided Markings

12) Repeat step 11 on the ceramic coupons.

13) With the Starlite diamond tipped drill bit and JET mill, drill 1.52 mm into the center of the ceramic, see Figure 3.28, 29, and 30.

I.   The ceramic and the mounting structure was kept submerged in a container of water to dissipate the heat from the drilling, see Figure 3.31

II.   Set the low speed to 150 and high to 1240, see Figure 3.32.

Figure 3.28. JET mill with Acru-Rite display

Figure 3.29. Acru-Rite Display Used to Control Location and Depth of the Drill Operation

Figure 3.30. Ceramic Coupon Being Drilled

Figure 3.31. Ceramic Coupon in a Holding Mount Submerged in Water

Figure 3.32. Speed Setting of the JET Mill

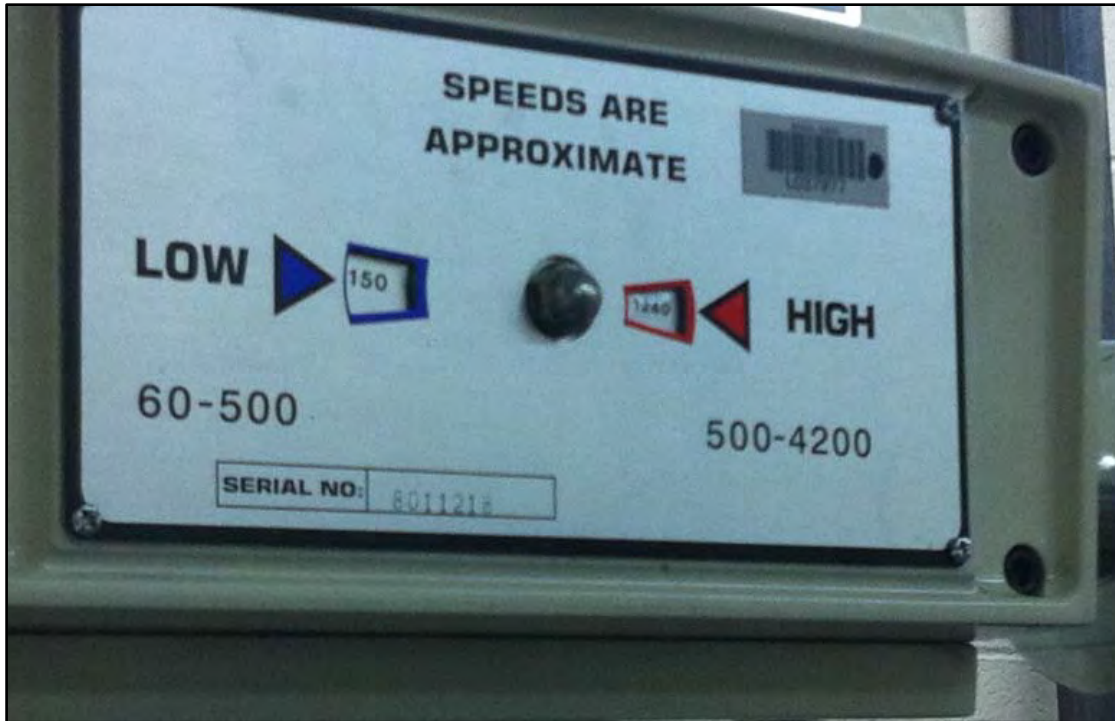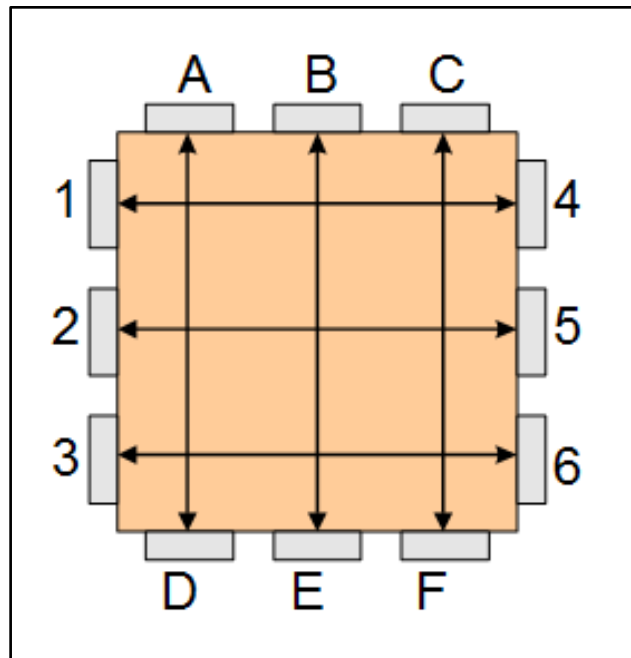15) Collect wave propagation data using the systematic pitch-catch technique shown on Figure 3.33.

Figure 3.33. Systematic Pitch Catch Technique

16) Repeat step 13 drilling to 3.04 mm.

17) Repeat step 14 to collect wave propagation data using the systematic pitch-catch technique.

18) Repeat step 13 drilling to 4.56 mm.

19) Repeat step 14 to collect wave propagation data using the systematic pitch-catch technique.

Anticipated Finding and Relevance

The anticipated findings will be optimal wave propagation settings to use (frequency, how many cycles of tone bursts, wave velocity). In addition, the wave propagation characteristics (time of travel and voltage amplitudes) on the materials individual, together, without damage and without damage will be understood. Importance of sensor placement locations will be analyzed. It would also determine if bulk waves could be used and also if it is possible for one sensor on each side of the coupons to be used to determine structural changes to two layers.

Ballistic Testing

Conducting a ballistic test of the actual panel produced by the manufacture, ArmorStruxx, is critical to predicting the actual feasibility of structural health monitoring of the two layers armor with ballistic damage.

Scope and Limitation

The main scope of the ballistic test is to continue on from David Fecko's. The type of ballistic projectile, velocity of projectile, angle of penetration, and ratio of ceramic to composite were carried on from Fecko's experiment. Active sensing was only evaluated. At the time, passive sensing was not possible due to lack of proper equipment.

Constraint and Boundaries

A major constraint for this portion of the experiment was the scheduling of the ballistic testing. Even though it was carried out on a ballistic range on Wright Patterson Air Force Base, it took over 10 weeks to finalize the availability of the ballistic range. The entire operation of the ballistic test was conducted by trained 46th Test Group personnel.

The ballistic experiment was conducted in a controlled and in-door laboratory, thus not being able to replicate environmental conditions that an armored HMMWV may encounter in Afghanistan or Iraq, which eliminates hundreds of possible random external inputs.

Due to the cost of the experiment and material, 12" x 12" test panels will be used instead of typical 24"x24" test samples required by (MIL-DTL-64154B). The cost comparison is $450 versus $1,800 for three panels.

A boundary set was to only experiment with the two layer systems (HJ1 composite with Al_2O_3 ceramic frontal plating). This excludes any other possible armor system used by the M1114 HMMWV. The other boundary was to use the V50 velocity of 948 meters/second instead of all the other possible V50 achievable with an AK-47 assault rifle using an armor piercing projectile. No other types of tactical weapons were be analyzed (e.g. improvised explosive devices, rocket propelled grenades, non-AP/AP projectiles of different calibers).

Equipment

- 46th Test Group Ballistic Range, see Figure 3.34-38

- o Wright Patterson Air Force Base, Ohio

- o Office Located in Bldg. 1661
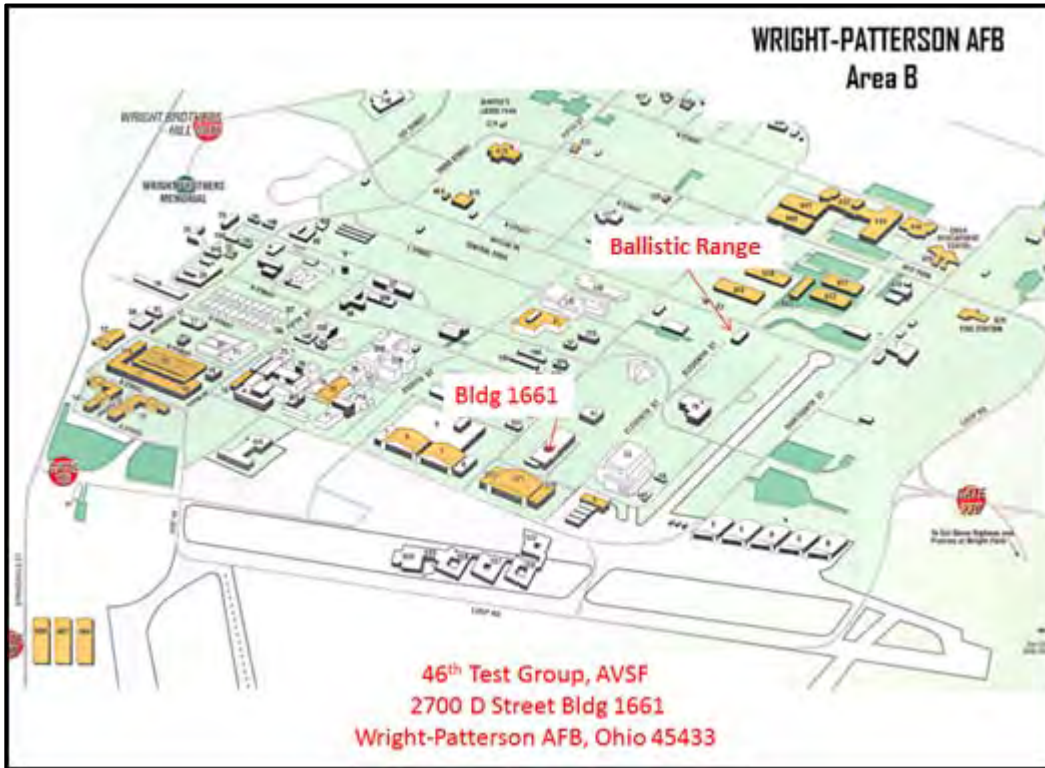
Figure 3.34. Location of 46th Test Group Ballistic Range
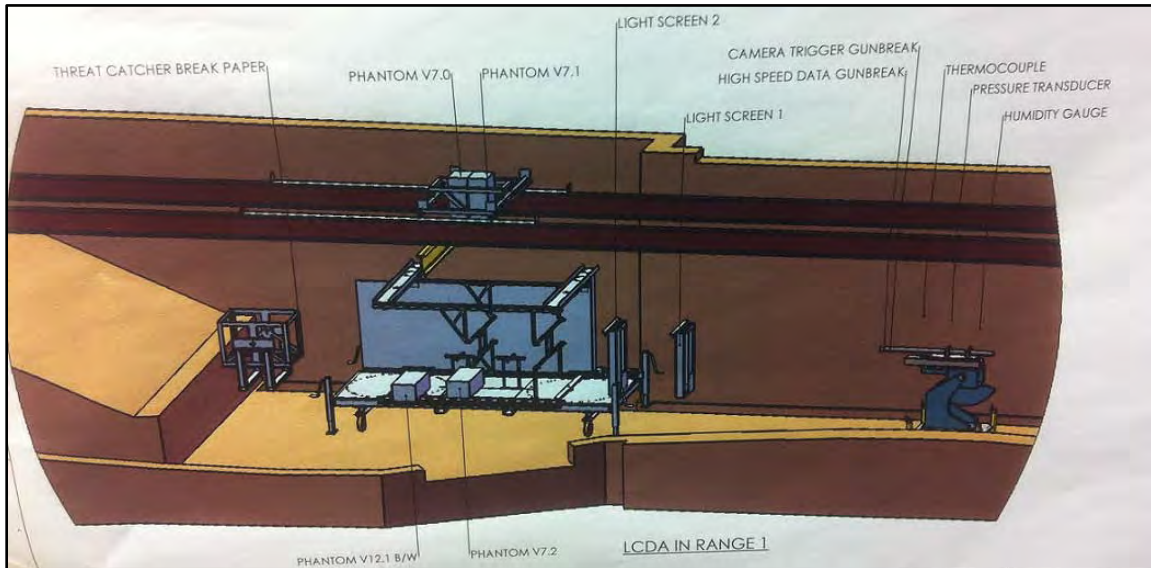
Figure 3.35. Schematic Layout of the Ballistic Range

Figure 3.36. Rear View of the Rifle and Target Area

Figure 3.37. Target area with the Target Mounting Structure
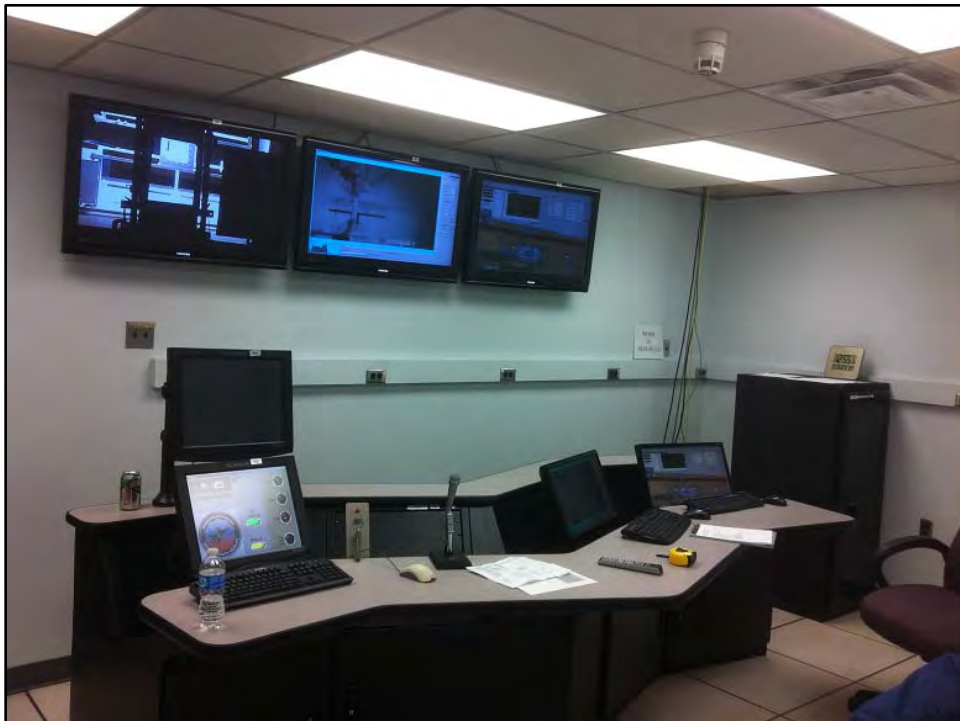
Figure 3.38. Control Room

- Two High Speed Cameras, Figure 3.39 and 40.

Figure 3.39. Side View Camera
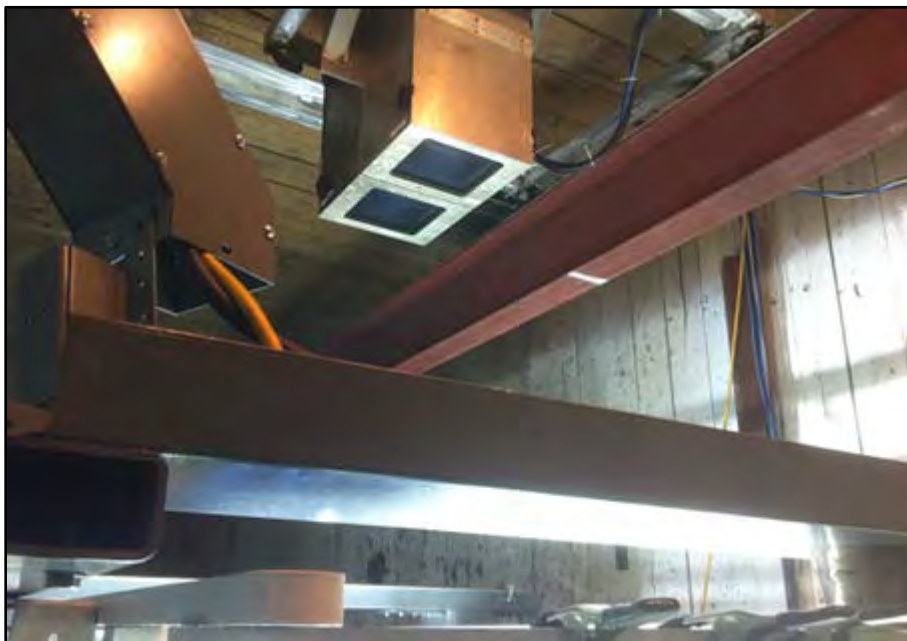
Figure 3.40. Top View Camera

- Remote triggered rifle, Figure 3.41 and 42.

Figure 3.41. Remote Triggered Rifle

Figure 3.42. Rear View of the Remote Triggered Rifle

- Two 30 cal (7.62 x 54 mm) Armor Piercing Projectiles, Figure 3.43

Figure 3.43. Projectiles

- Four C-clamps, Figure 3.44

Figure 3.44. C-clamp

- 12" x 12" HJ1 Composite with Ceramic Face Armor, Figure 3.45
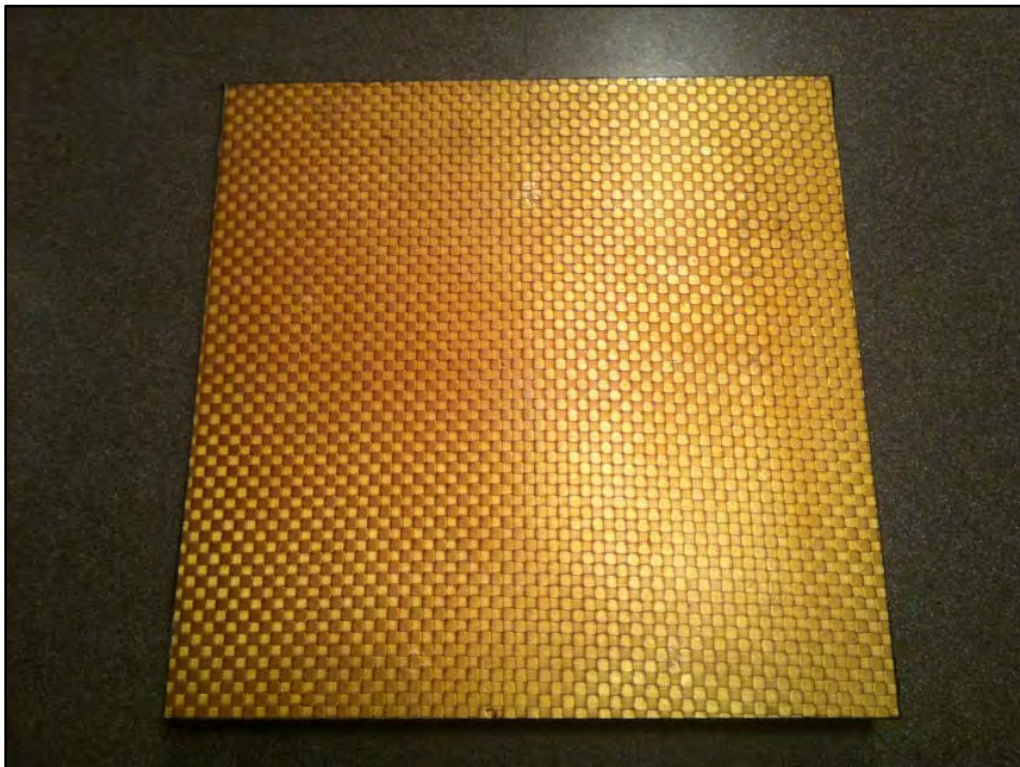
Figure 3.45. Two Layer Armor From ArmorStruxx

- 12" x 12" Aluminum Plate to conduct equipment check test fire

- Timing cable placed on the barrel end of the rifle

    o Captures start time of projectile travel when projectile breaks the cable

- Timing sheets

Validity

Internal validity of the experiment is demonstrated by applying cause and effect studied from the prior base line experiment and Fecko's experiment. The experimental procedures were cloned from Fecko's experiment, thus replicability is possible.

Independent Variables

- Velocity of projectile

- Type of projectile

- Strike angle of projectile

- Strike location on armor

Dependent Variables

- Impact damage on the armor

Procedure (conducted by trained 46th Test Group personnel)

1) Connect all the cable for the cameras to function.

2) Place the equipment check aluminum sheet onto the slots on the firing mount structure.

3) Place the timing sheet on the aluminum plate.

4) Place the timing cable on to the barrel end of the rifle.

5) Place a 30 cal armor piercing projectile into the rifle.

6) Conduct final equipment checks of cables and rifle.

7) Secure the firing range by closing the access door from the control room to the firing range.

8) Remote fire the test projectile.

9) Once the range has been cleared, remove the aluminum test sheet from firing mount structure.

10) Inspect the rifle to be clear and ready for use.

11) If test fire was a success, continue on to setting up ballistic test on the two layer armor.

12) Place the two layer armor on to firing mount structure and use the four c-clamps to hold in place. See Figure 3.46 and 47.

Figure 3.46. 46th Test Group Personnel Clamping on the Armor System

Figure 3.47. Another View of the Set Up

13) Make sure that the strike face of the armor is place in the correct direction

14) Place the timing sheet on the mount as shown on Figure 3.48.

Figure 3.48. Location of where the Timing Sheet is Placed

15) Place the timing cable on the barrel end of the rifle.

16) Place a 30 cal armor piercing projectile into the rifle.

17) Conduct final equipment checks of cables and rifle.

18) Secure the firing range by closing the access door from the control room to

the firing range

19) Remote fire the test projectile.

20) Once the range has been cleared, remove the armor from firing mount

structure.

Anticipated Findings and Relevance

Anticipated findings were that the ballistic experiment and damage findings will

be similar to Fecko's findings during his experiment. With the armor that has actually

been ballistically damaged, it can be used to conduct NDE evaluation experiments. The

armor system now can be determined if SHM is feasible. Once the NDE evaluation has

been conducted and proven that it works, tomographic modeling can be conducted. This

will enable a vehicle inspectors, operators, convoy commanders, and operations

commanders to remotely monitor the structural integrity a vehicle or the entire fleet. It

would theoretically provide a system that would enable anyone to remotely detect, locate,

and quantify structural damage.

IV. Results and Discussion

Individually Base Line Testing of Ceramic Coupons

Wave propagation data collected using longitudinal transducers individually for the alumina ceramic coupons correlated well to its physical properties. The initial time of arrival is at 0.000007 seconds for the entire frequency range from 300 KHz to 1000 KHz. The max peak to peak started at 2.23 mV at 300 Hz and increased to 15.87mV at 1000 KHz. The overall characteristic is of low attenuation of but very complex wave signals, Figure 4.1. These characteristics can be attributed to the ceramic's high mechanical strength, hardness, high wear resistance, and stiffness. All of these attributes will enable high velocity and short duration for signal capture. The residual wave propagation starting at 0.00002 seconds is the waveguide effect created from the limited thickness of ceramic coupon compared to the oversized transducer (ratio of two to one). The overall signal characteristics were enhanced as frequency was increased. Transverse transducers were also used but did not produce significant data compared to the longitudinal transducers.

Figure 4.1. Wave Propagation of Ceramic Coupon #4

Individually Base Line Testing of HJ1 Composite Coupons

Wave propagation data collected using longitudinal transducers on the individually HJ1 composite coupons also correlated well to its physical properties. The initial time of arrival is at 0.000013 seconds for the entire frequency range from 300 KHz to 1000 KHz. This is much later compared to the ceramic coupons. The max peak to peak started at 5.06 mV at 300 Hz peaks at 6.99 mV at 400 KHz and steady drops back down to 3.7 mV at 1000 KHz. The overall characteristic is of simpler and cleaner wave propagation compared to ceramic with higher attenuation, Figure 4.2. These characteristics can be attributed to the composite's ability to absorb energy. There was more attenuation due to consolidation of wave signals instead of scattering of energy. There was no waveguide effect due to increased thickness level compared to the ceramic.

67

There also was enhanced level of propagation at lower frequency (300 – 500 KHz).

Transverse transducers were also used but did not produce significant data compared to
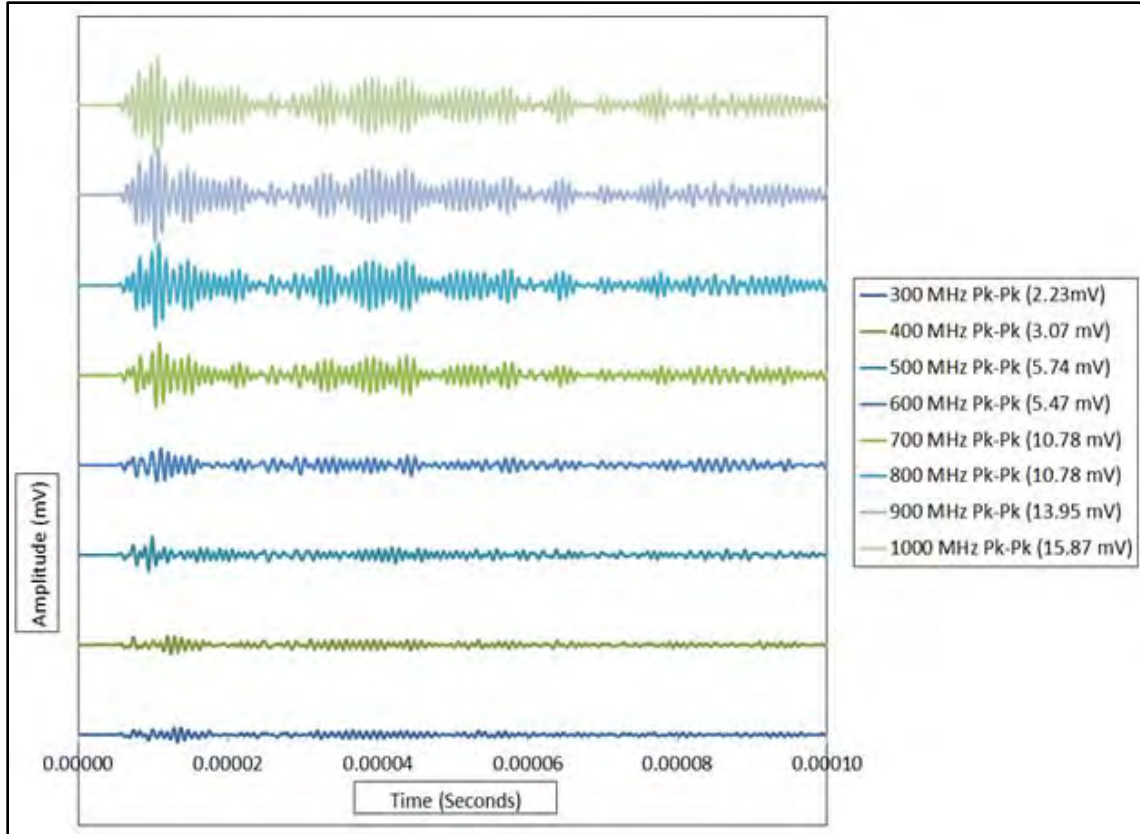
the longitudinal transducers.
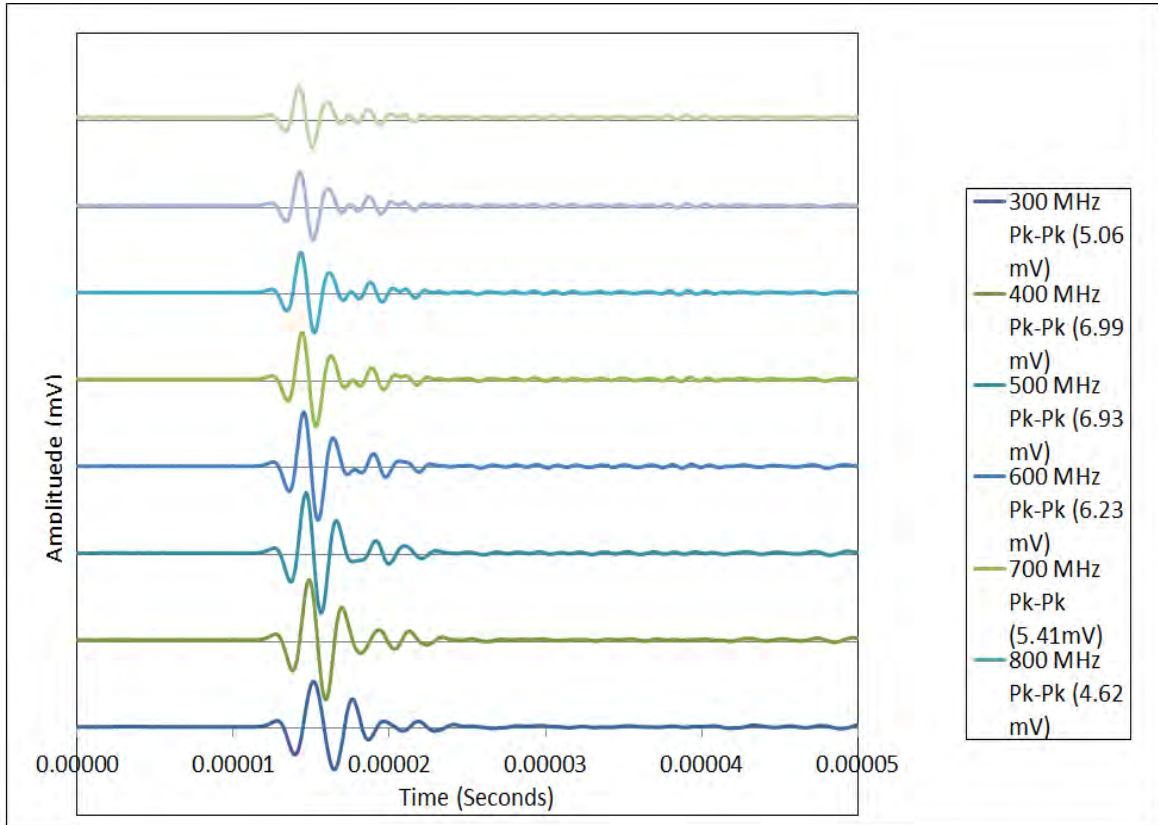
Figure 4.2. Wave Propagation of HJ1 Composite Coupon #4

Combined Base Line Testing of HJ1 Composite and Ceramic Coupons

Wave propagation data collected with the HJ1 composite and ceramic coupons

clamped together is shown on Figure 4.3. The wave propagation in the lower 300-500

KHz range reflects those of the HJ1 composite, but those of the ceramic coupons in the

higher 600-1000 KHz range. In the 300-500 KHz range, majority of the wave

propagation starts at 0.000013 and there are minimal residual waveguide effects. In the

600-1000 KHz range, attenuation starts at 0.000006 seconds (similar to the individually

tested ceramic coupons). There is also significant amount of waveguide effects in this

range of frequency. From this analysis, 600 KHz was determined to be the optimal

frequency to use to capture structural changes on both materials using only one sensor per

side on both materials, instead of ones set of sensor on each sides of the material. 600

KHz was chosen because the wave propagation reflects both properties of the ceramic

and the composite see Figure 4.4.
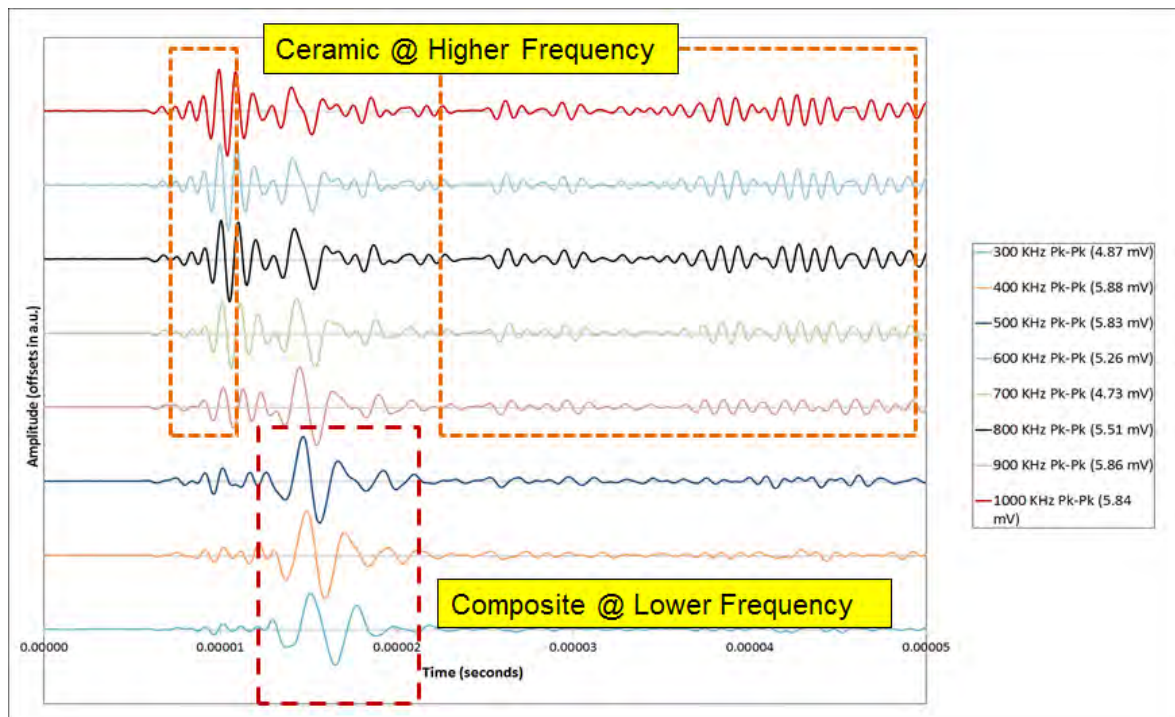
Figure 4.3. Wave propagation of Ceramic Coupon #4 and HJ1 Coupon #4 in 300-1000
KHz
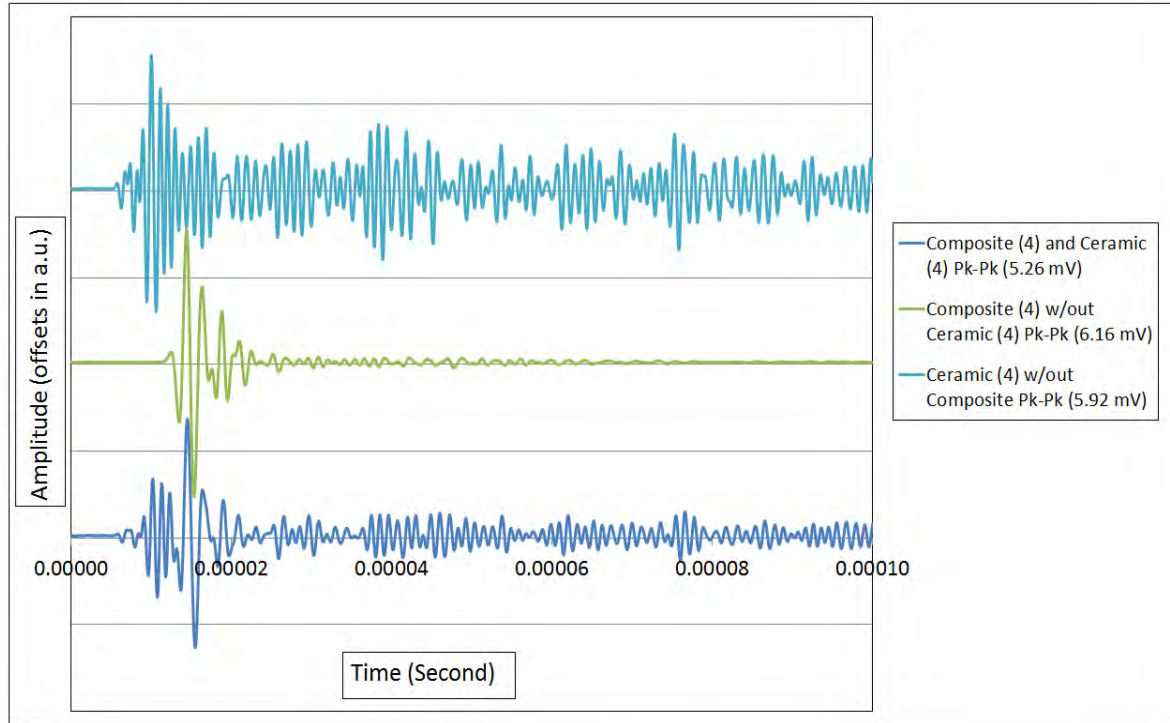
Figure 4.4. Wave Propagation Comparison of only Ceramic, HJ1 Coupon, and the Two Together at 600 KHz

Combined Base Line Testing of HJ1 Composite and Ceramic Coupons with No Damage

The wave propagations on Figure 4.5 are of those using 300-1000 KHz with the ceramic coupon and composite coupons clamped together. Figure 4.5 will be used as a base line comparison to ceramic and composite combos with different amounts controlled damages.
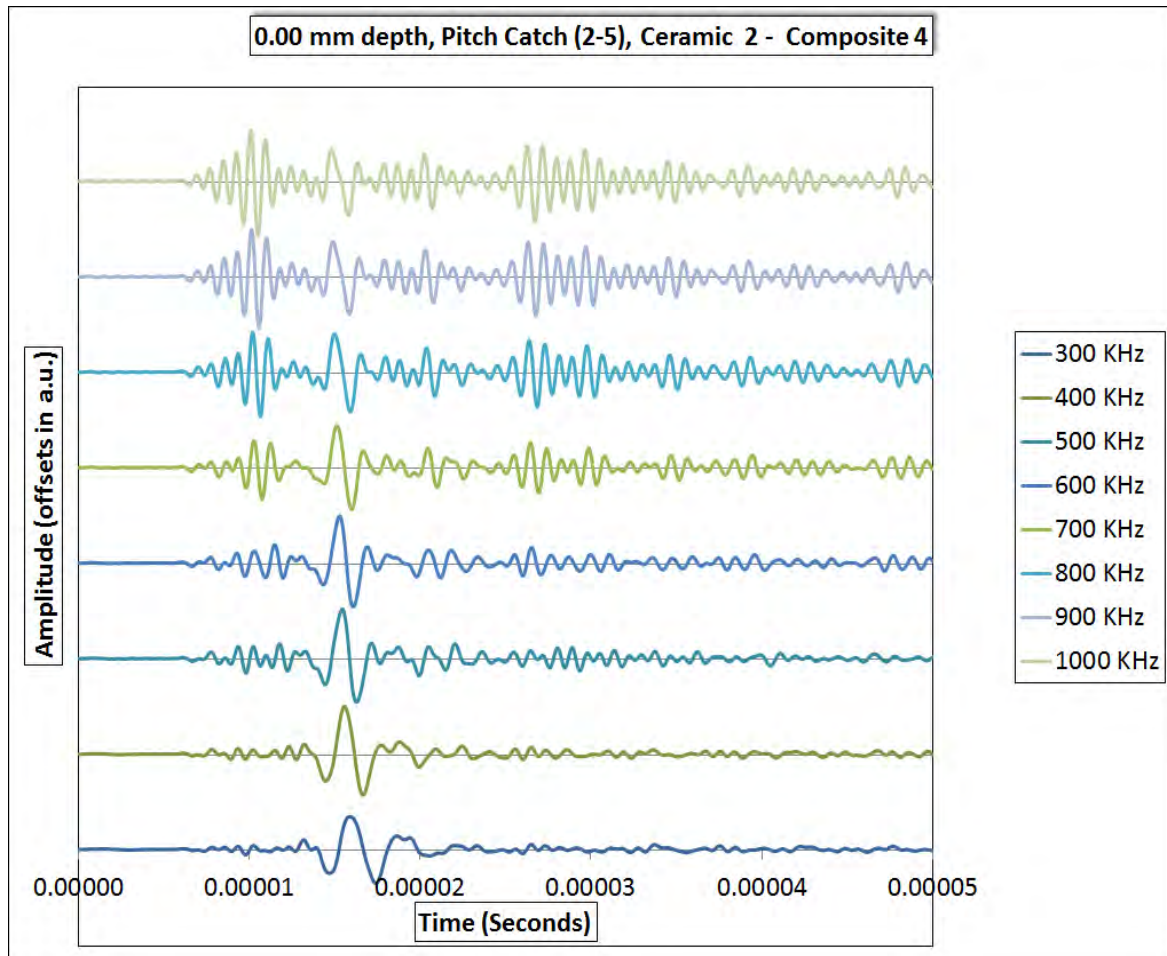
Figure 4.5. Wave Propagation from 300 KHz to 1000 KHz With No Damage, Pitch Catch from Section 2 to 5

Combined Based Line Testing of HJ1 Composite and Ceramic Coupons with 1.6 mm Depth of Damage

The wave propagations on Figure 4.6 are of those using 300-1000 KHz with the ceramic coupon and composite coupons clamped together, with a controlled circular hole (3.13 mm diameter) drilled 1.6 mm into the ceramic. The overall characteristic is consistent throughout the 300 to 1000 KHz range. This would indicate that input frequency changes will not affect the data capture and analysis of the structural change that has occurred.

71

Figure 4.6. Wave Propagation with Damage at 1.52 mm Depth from 300 KHz to 1000 KHz

Combined Based Line Testing of HJ1 Composite and Ceramic Coupons with 3.04 mm depth of Damage

The wave propagations on Figure 4.7 are of those using 300-1000 KHz with the ceramic coupon and composite coupons clamped together, with a controlled circular hole (3.13 mm diameter) drilled 3.04 mm into the ceramic. The overall characteristics are very different from those with 1.6 mm depth damage. There is a lot of wave propagation shown that makes it difficult to discriminate for any indicators. Waveguide effect is very high with the 3.04 mm depth damage. This could be due to inconsistent alignment of sensors from one experimental procedure to the other. It could be due to inconsistent flushness of the two materials sharing the sensor producing false wave propagation. At

72

least within this procedure step, the overall characteristic is consistent throughout the 300 to 1000 KHz range.
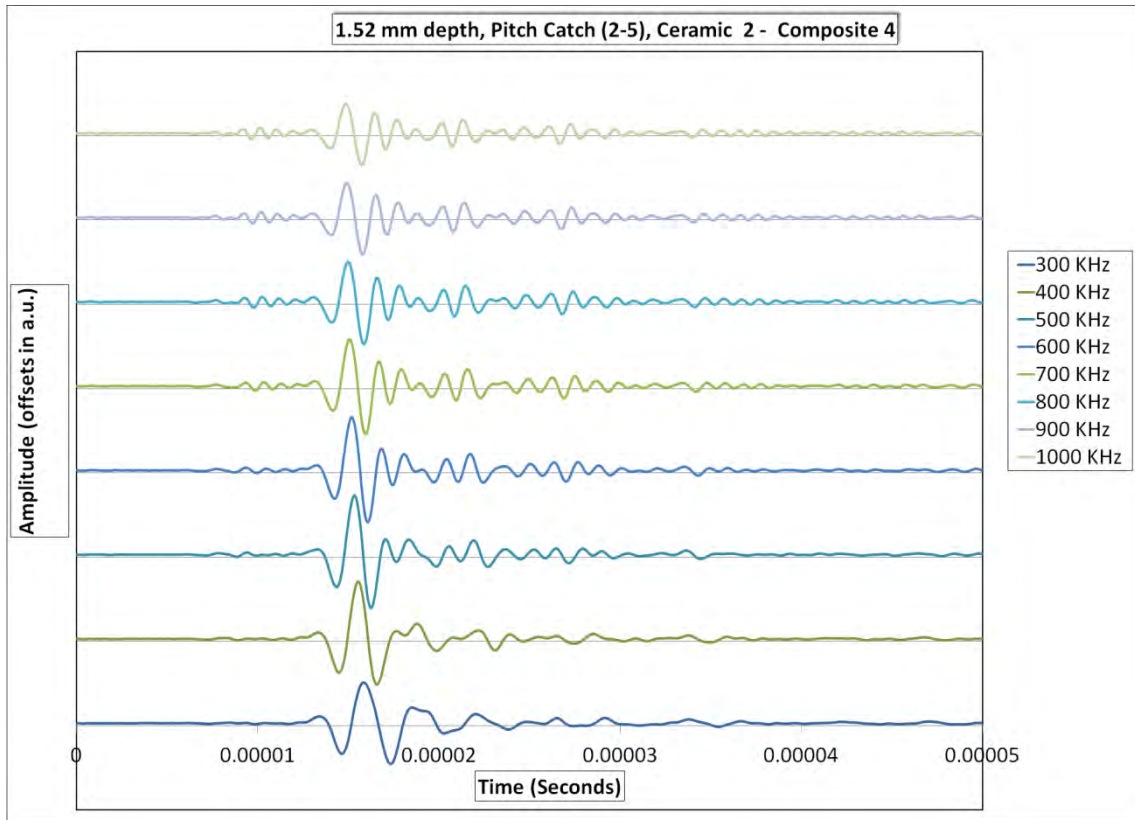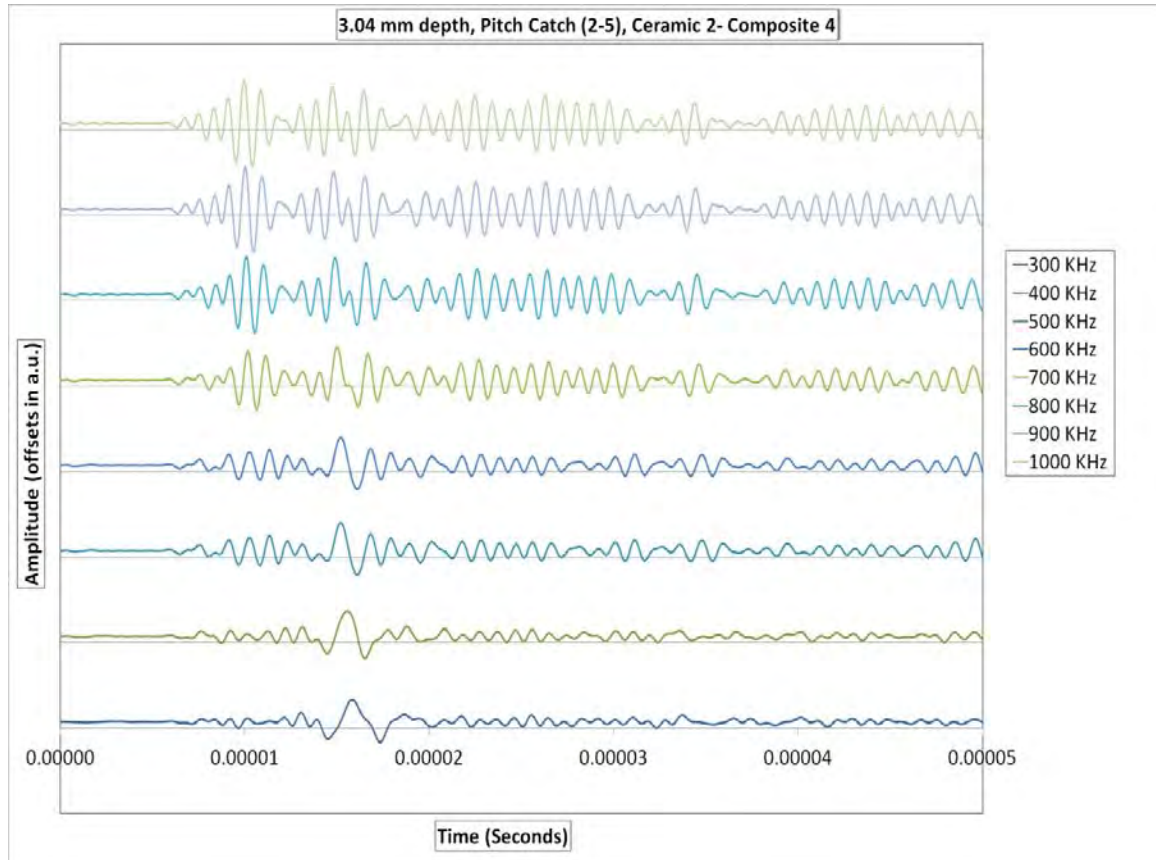

Figure 4.7. Wave Propagation with Damage at 3.04 mm Depth from 300 KHz to 1000 KHz

Combined Based Line Testing of HJ1 Composite and Ceramic Coupons with 4.56 mm depth of Damage

The wave propagations on Figure 4.8 are of those using 300-1000 KHz with the ceramic coupon and composite coupons clamped together, with a controlled circular hole (3.13 mm diameter) drilled 4.56 mm into the ceramic. The overall characteristic is consistent throughout the 300 to 1000 KHz range. Figure 4.8 is very similar to Figure 4.6. This indicates there is correlation between the type of damage introduced and what type

of changes to wave propagation to investigate. This also confirms that it can be

replicable.
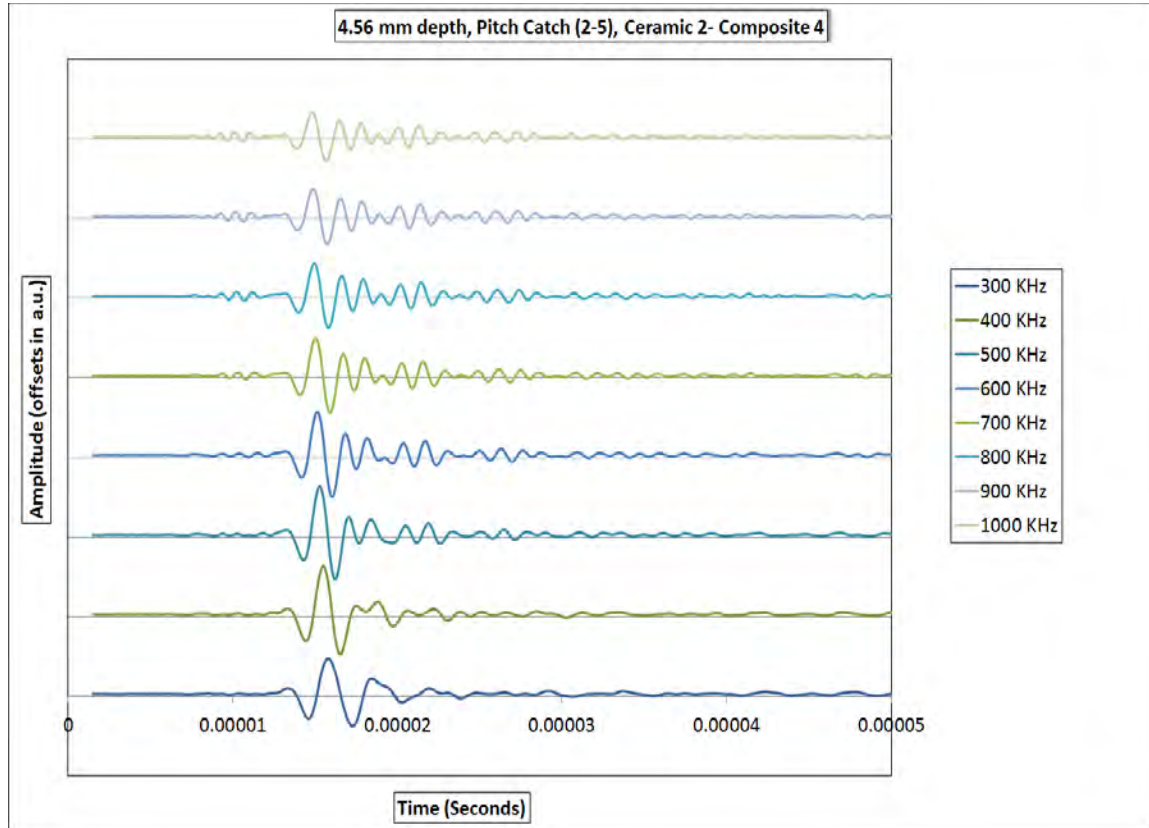
Figure 4.8. Wave propagation with damage at 4.56 mm depth from 300 KHz to 1000 KHz

Analysis of the Different Damage Depth

The graph on Figure 4.9 is a compilation of those with no damage and damage

introduced by a 3.13 mm circular diamond bit milled into the ceramic frontal plate at 1.56

mm, 3.04 mm, and 4.56 mm at 600 KHz. Key features are indicated with the dashed

boxes. First key feature to notice is at 0.000015 second range, the wave propagation

during this time frame is very close to being the same for no damage, 1.52 mm, 3.04 mm,

and 4.56mm. This key feature concludes that the sensors indicated no change to the

structural properties for the composite coupons. Second key feature reflects the structural

changes that have occurred due to the controlled damage that has been placed on the ceramic coupons. There is a decrease of attenuation in the early (0.000007 second) and residual region of the wave propagation. This supports the fact that was a loss of capturing wave propagation due to the waves reflecting off the structural boundary introduced by the damage.

With the extraction of these two key features, it can be concluded that one set of pitch-catch sensors can be used to evaluate a two layer interface. In extension, this also proves that bulk waves can be used to evaluate structural changes in between a volume of material.

The data collected from 3.56 mm depth of damage is not similar to those of other damage depth and no damage. This can only be from difference in experimental setup. This could be from non-even flushness of the ceramic and composite coupons. The errors could also come from imperfect alignment of sensors.
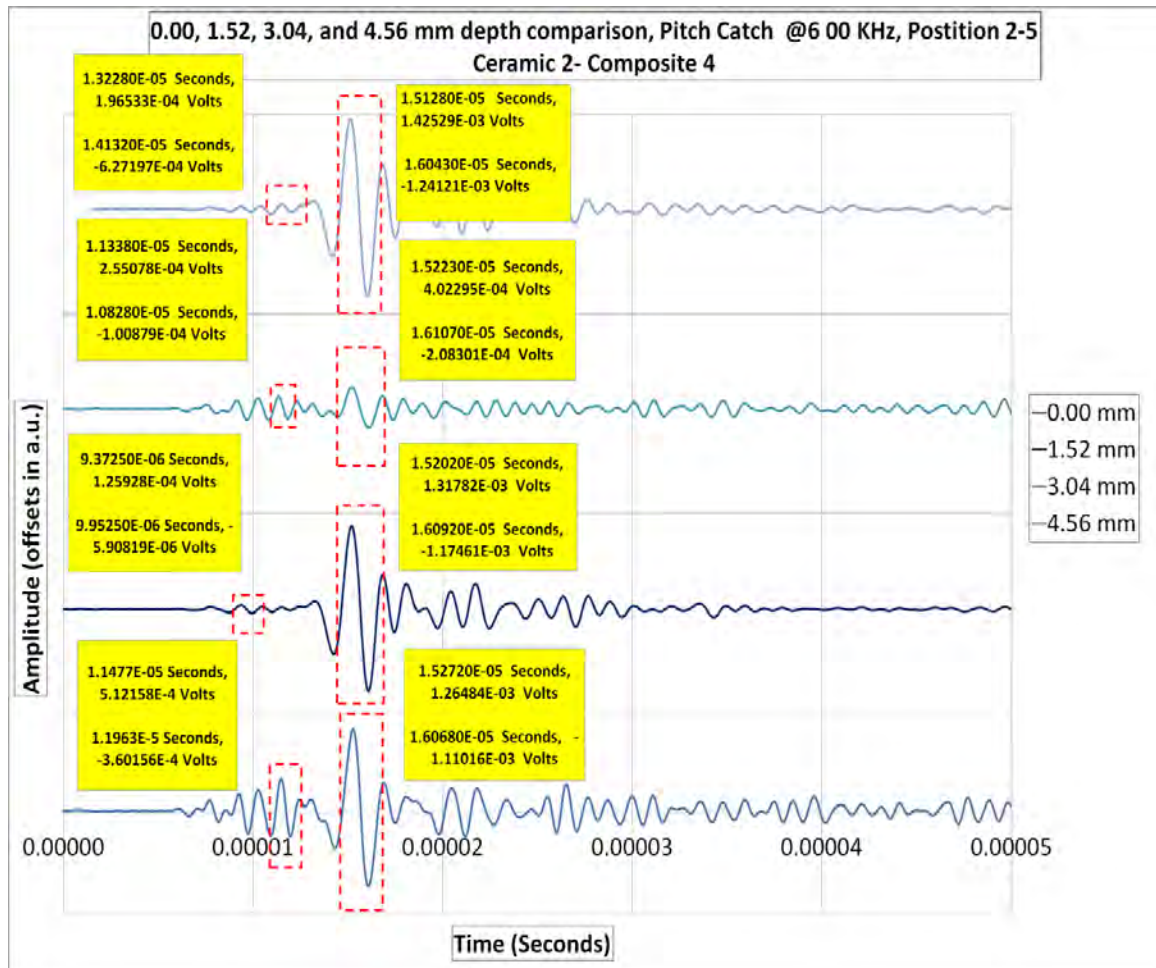
Figure 4.9, Wave Propagation Compilation of all Damage Amounts At 600 KHz

Equipment Check on the Sheet of Aluminum

The equipment test fire on the sheet of aluminum was a success, see Figure 4.10. The test fire ensured that the slow motion cameras and the timing system were functioning properly. The target was struck dead center mass and at a zero degree angle of strike. The test did indicate that the maximum achievable velocity for the ballistic range was 834.8 meters/second instead of the goal of reaching 948 meters/second.

Figure 4.10. Successful Test Fire for Equipment Check

Ballistic Test Fire

The ballistic was successful just like the test fire. The two layer armor in Figure 4.11 was struck center mass with a zero degree angle of strike. The ceramic frontal plate functioned as it was designed to do so. The ceramic's high mechanical strength, hardness, and stiffness absorbed the majority of the kinetic energy from the armor piercing projectile. The ceramic's structural integrity breaks as it deforms the tungsten core of the projectile. The HJ1 composite absorbs and dissipates the remaining energy in the layered structure of the composite. There is a bulge on the back side of the armor system, but there was no penetration through the HJ1 composite. Figures 4.12 -15 provides a top view of the ballistic impact testing. Figures 4.16 -19 provides a top view of the ballistic impact testing.

Figure 4.11. Successful Ballistic Test on the Two Layer Armor

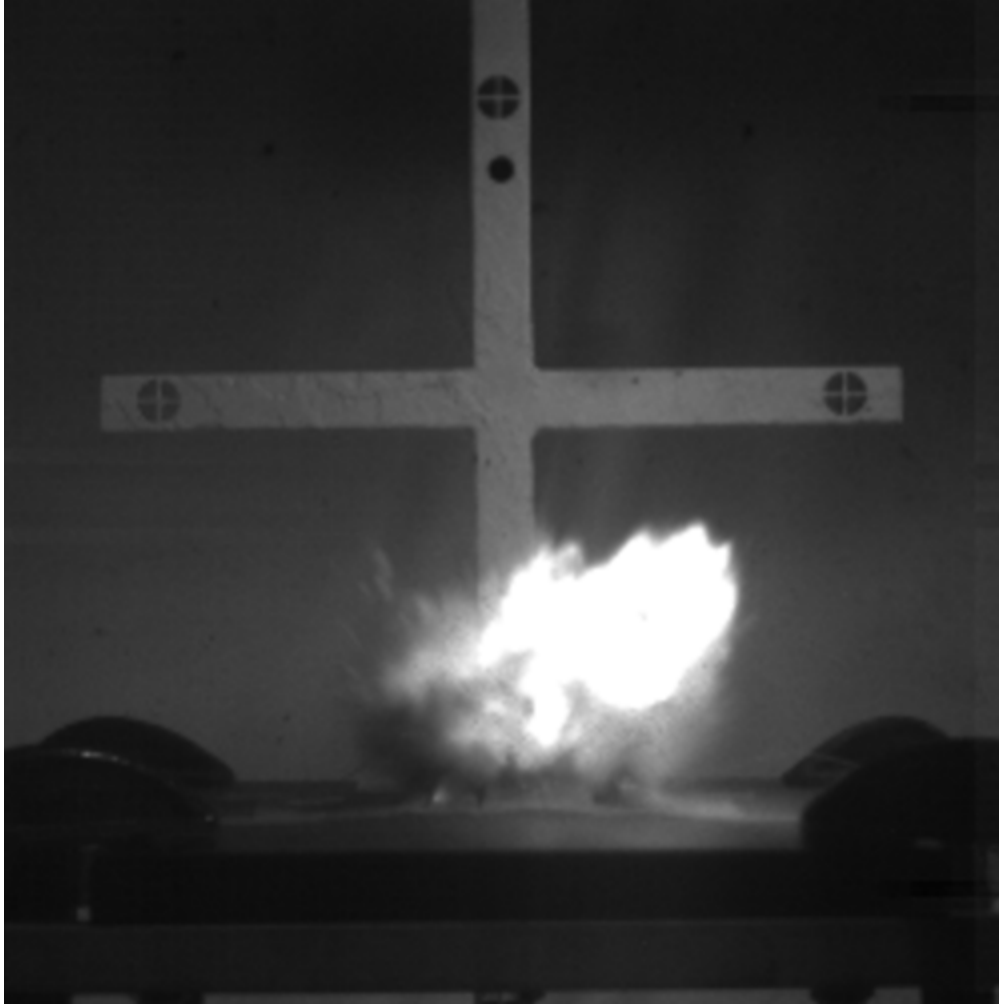Figure 4.12. Top View of the Projectile Before Impact
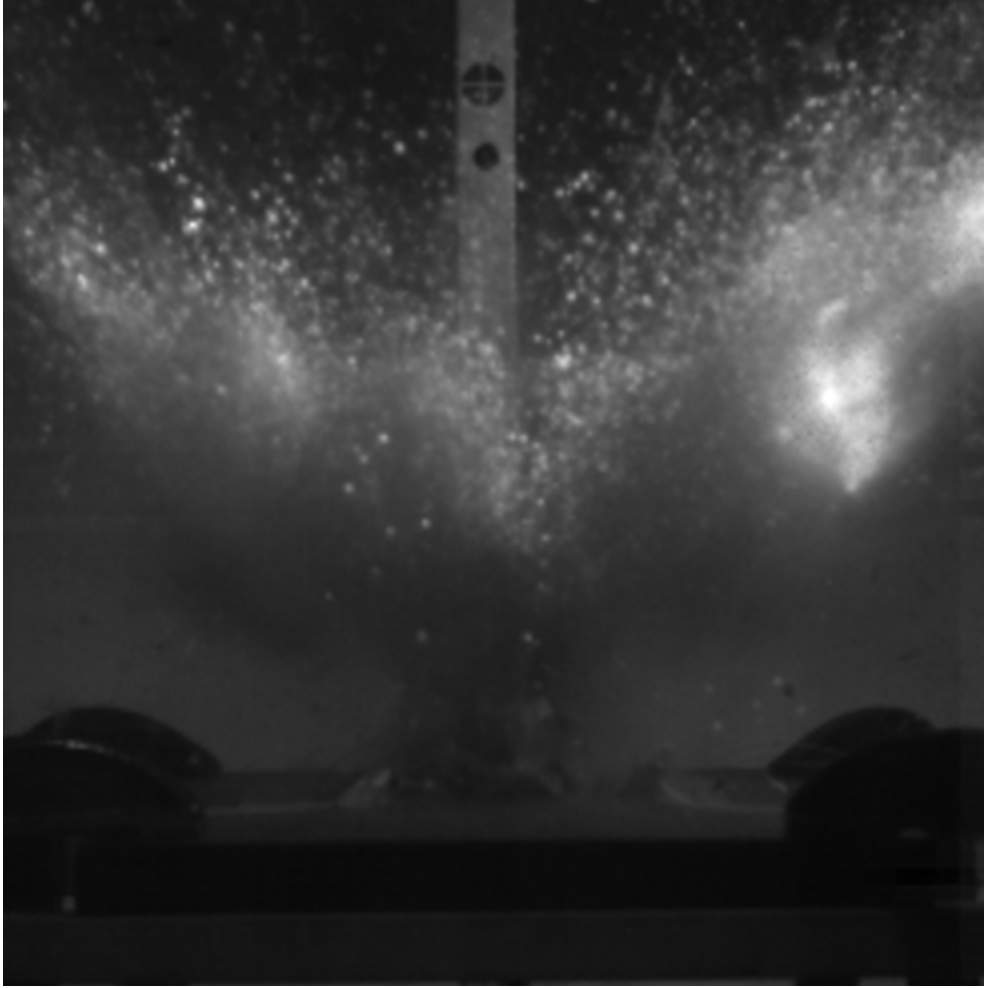
Figure 4.13. Top View of Impact

Figure 4.14. Top View of the Ceramic Debris Fallout
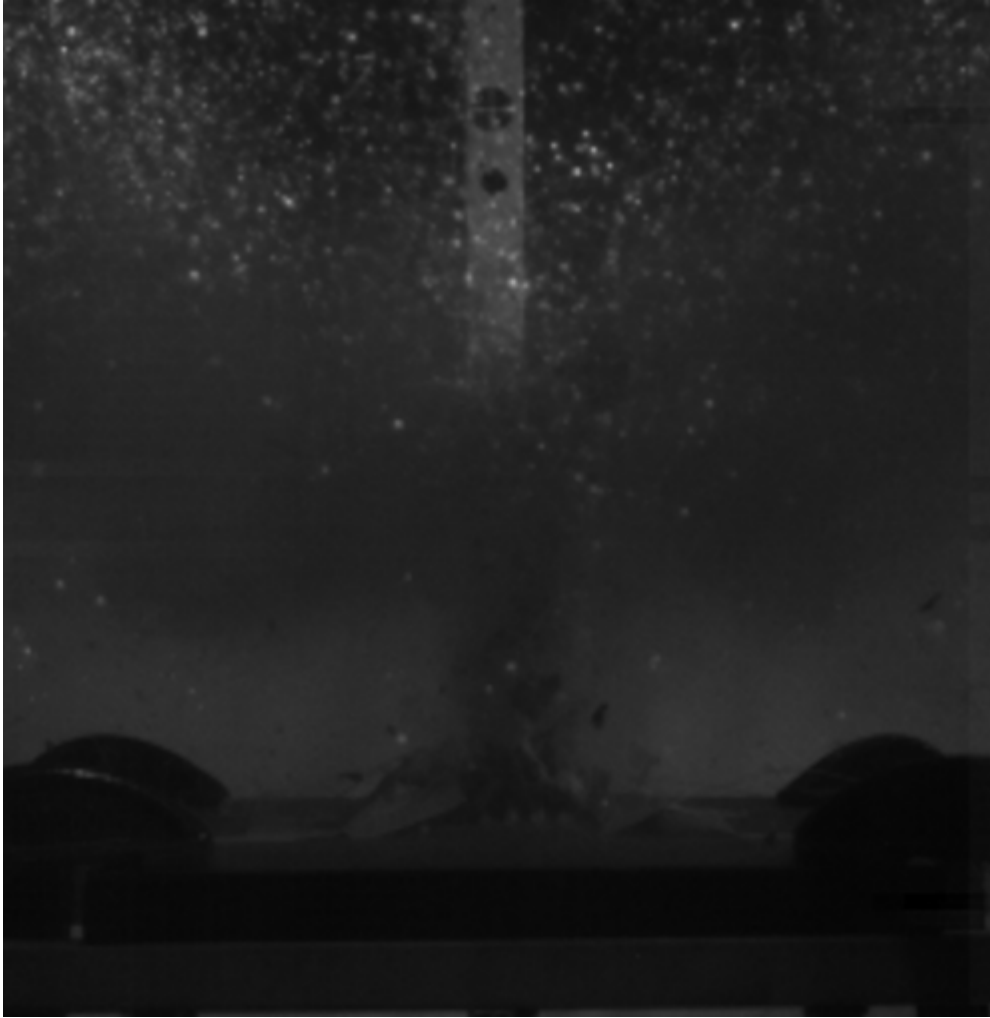
Figure 4.15. Top View of the Ceramic Structural Cracking

Figure 4.16. Side View of the Projectile Prior to Impact
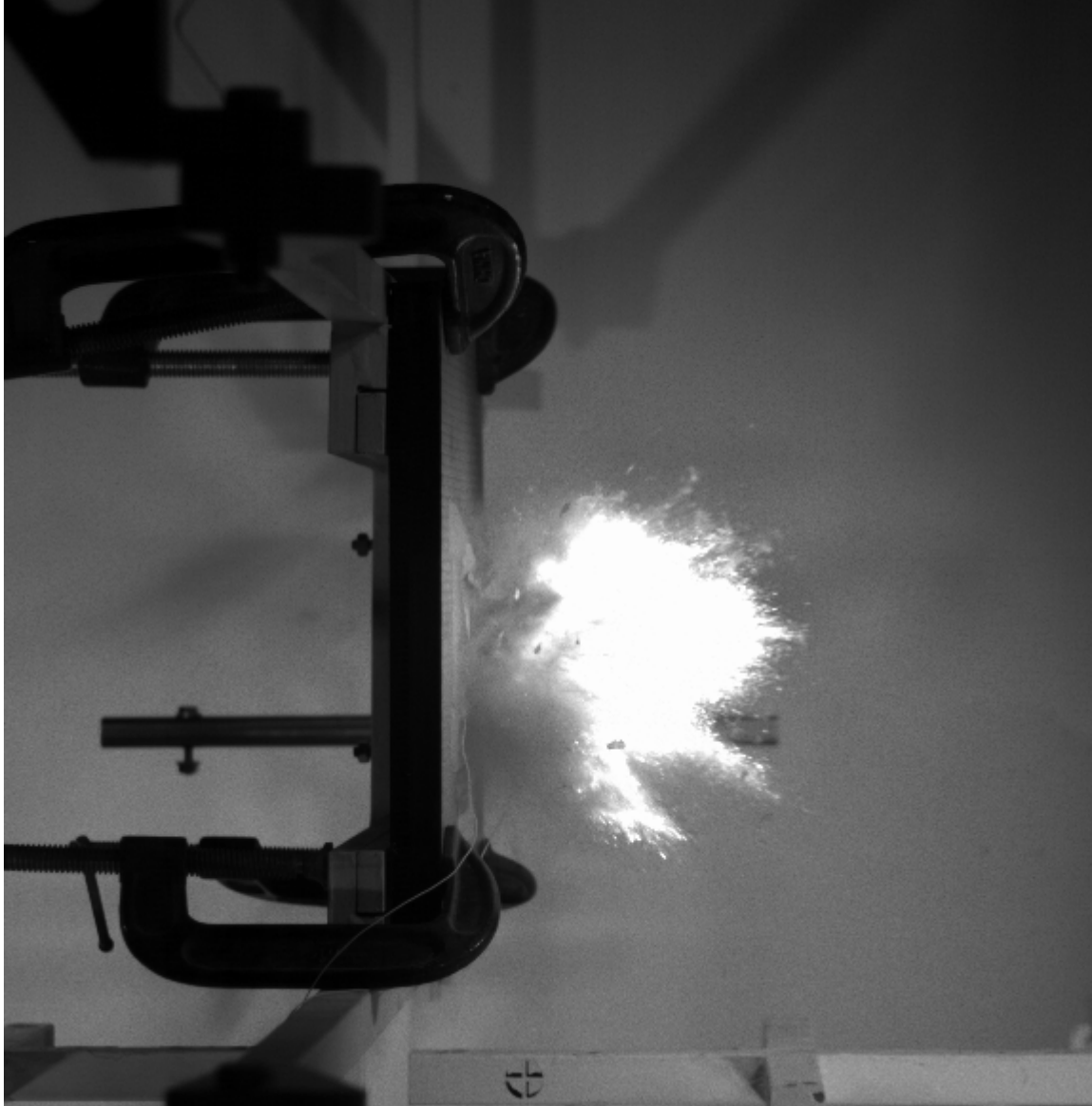
Figure 4.17. Side View of the Impact
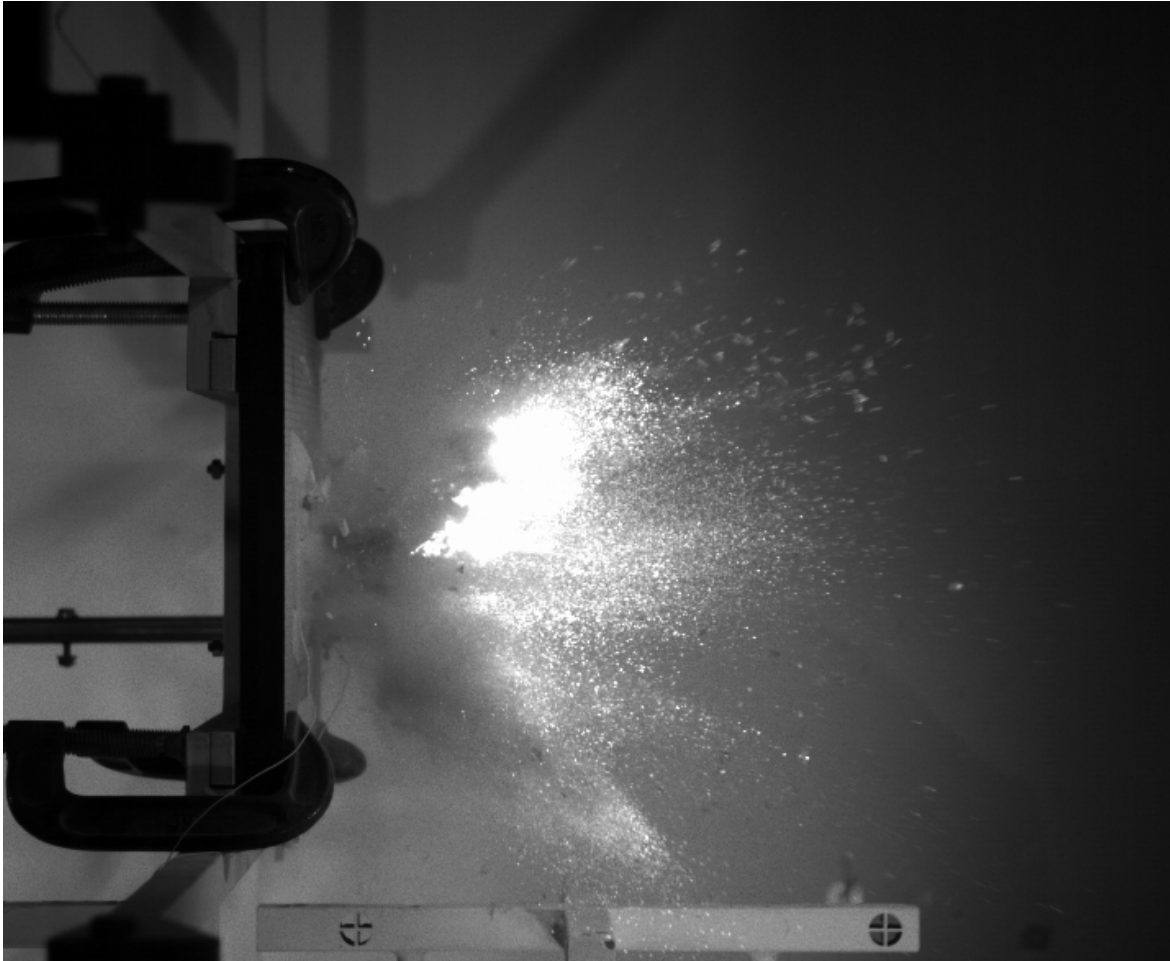
Figure 4.18. Side View of the Ceramic Debris Fallout
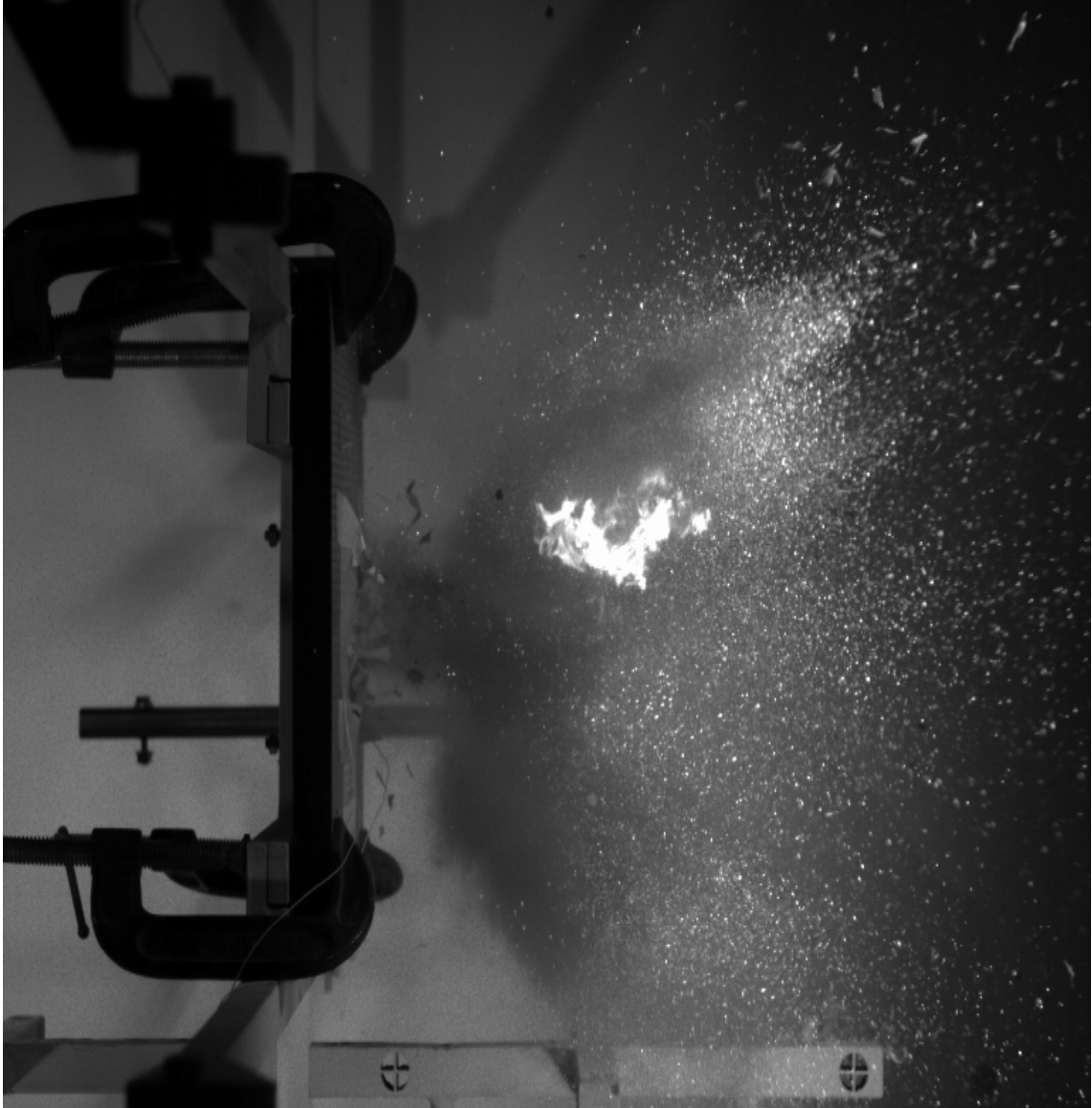
Figure 4.19. Side View of the Ceramic Structural Cracking

V. Conclusion

Through the experiments conducted, I concluded that the hypothesis set forth in the methodology was proven to be truth. Non-Destructive Testing Evaluation through Structural Health Monitoring is possible by detecting, locating, and quantifying amount of damage on the two layer armor system. It was found through experimental process, that longitudinal transducers using longitudinal waves were proven to work. Maintaining a high number of sensors is important, because if the structural damage on the armor is not on the path of the wave propagation, it can reduce attenuation. Data acquisition and evaluation was proven to work with only one sensor per side of two layers of materials.

All the founding's conducted on individual panels tested individually and mechanically clamped together. Further NDT evaluation needs to be conducted on the armor panels produced from ArmorStruxx that was actually ballistically damaged.

Bibliography

All Departments and Agency of the Department of Defense. Detail Specification. Laminate: Fiberglass-Fabric-Reinforced, Phenolic. MIL-DTL-64154B. *Washington: Department of Defense*, 17 December 2008.

Brush, E.R., D.E., Adams, Zwink, B.R., & Walsh, S. (2009). Passive health monitoring coupled with full-field active inspection of multi-layered composite armor structures. *Review of Quantitative Nondestructive Evaluation* Vol.28.

Dawson, B. (1976). Vibration condition monitoring techniques for rotating machinery. *The shock and vibration digest*, 8(12).

Department of Defense. Department of Defense Test Method Standard. V50 Ballistic Test for Armor. MIL-STD-662. *Washington: Department of Defense*, 18 December 1997.

Department of Defense. Operator's Manual for M1114 HMMWV Vehicle. TM 9-2320-387-10-HR. *Washington: Department of Defense*, 2009

Donaldson, J. S. (2010). Computed tomography. Retrieved from *http://www.childrensmemorial.org/depts/radiology/ctscanprocedure.*

Emergency supplemental appropriations act for defense, the global war on terror, and tsunami relief, 2005. (n.d.*). Retrieved from http://www.govtrack.us/congress/bill.xpd?bill=h109-1268*

Fecko, D., Douglas P., Murray, D.(2002). The Synergistic Roles of High Strength Glass Composite and Alumina Ceramic Facing in Light Weight Composite Armor Against Armor Piercing Projectiles, *Technical Report.*

Gautschi, G. (2002). Piezoelectric sensorics, force, strain, pressure, acceleration and acoustic emission sensors, materials and amplifiers. Springer Verlag.Retrieved from *http://books.google.com/books/feeds/volumes?q=9783540422594*

Grujicic, M., Panduranga, B., Zecevic, U., Koudela, K. L., Cheeeseman, B.A. (2006). Ballistic Performance of Alumina/S-2 Glass Reinforced Polymer-Matrix Composite Hybrid Lightweight Armor Against Armor Piercing (AP) and Non-AP Projectiles, *Multidiscipline Modeling in Material and Strength*, Vol XX No. XX pp. (1-28).

Hall, S.R. (1999). The Effective Management and Use of Structural Health Data. Proceedings of the *2nd InternationalWorkshop on Structural Health Monitoring*, 265-275.

Hartman, D. R. (1986). Ballistic Impact Behavior of High-Strength Glass-Fiber Composites, 41th Annual Conference, *Reinforce Plastics Institute*, Session 16-D, 1-5 January 1986.

Ion, C. (2004). Objective comparision of design of experiments strategies in design and observations in practice. Unpublished manuscript, Engineering Systems Division, Massachusetts Institute of Technology, Massachusetts. *Retrieved from http://hdl.handle.net/1721.1/33163.*

Kesseler, S.S., Spearing, S. M., Soutis, C. (2001). Structural Health Monitoring in Composite Materials Using Lamb Wave Methods. *ASC-2001 #043.*

Kesseler, S.S., Spearing, S. M., Soutis, C. (2001). Damage Detection in Composite Materials Using Lamb Wave Methods. *Master's Thesis, Massachusetts Institute of Technology, Cambridge, MA.*

Kessler, S., Spearing, M., & Soutis, C. (2002). Damage detection in composite materials using lamb wave methods. Smart Materials and Structures, 11(2).

Kim, S., Pakzad, S., Culler, D., Demmel, J., Fenves, G., Glaser, S., & Turon, M. (2007). Health monitoring of civil infrastructures using wireless sensor networks.

Klein, R. (2004). Soldiers headed to iraq grill rumsfeld. *Boston Globe*

Langford, J., Gray, W. (1989). Composite Armor, in Concise *Encyclopedia of Composite Materials*, Pergamon Press pp 55-62.

Lissenden, C., Rose. (2008). Structural Health Monitoring of Composite Laminates Through Ultrasonic Guided Wave Beam Forming. RTO-MP-AVT-157. *NATO Research and Technology Oragnisation.*

Li, X., & Sun, L. (2011). Structure health monitoring data analysis for donghai bridge. Paper presented *at The 6th international workshop on advanced smart materials and smart structures technology*, Dalian, China.

Leonard, K. R., Malyarenko, E. V., & Hinders, M. K. (2002). Ultrasonic lamb wave tomography. Inverser Problems, 18(6).

Middendorf, W. (1986). Design and Devices and Systems, New York: Marcel Decker.

Na. J.K., Blackshire, J. L., Kuhr, S.L (2009). Detection of Surface Breaking Fatigue Crack on a Complex Aircraft Structure with Rayleigh Surface Wave.

Na. J.K., Blackshire, J. L., Kuhr, S.L (2009). Interaction of Rayleigh Waves Induced by Interdigital Transducer with Fatigue Crack. *Health Monitoring of Structural and Biological Systems*, vol. 7295.

Na. J.K., Blackshire, J. L., Kuhr, S.L (2009). Interaction of Rayleigh Surface waves with a tightly closed fatigue crack. *NDT&E International.*

Nondestructive Testing Handbook, Third ed.: Volume 7, Ultrasonic Testing. Columbus, OH: *American Society for Nondestructive Testing.*

Royer, R.L., Van Velsor, J., Rose, L. (2009). An Ultrasonic Guided Wave Tomography Approach for Pipeline Health Monitoring. Penn State University.

Russell, D (1999). Longitudinal and Transverse Wave Motion. Kettering University Applied Physics.

Stites, N. (2007). Minimal Sensing and Semi-Active Load and Damage Identification Techniques for Structural Components. Master's Thesis, Purdue Univiersity.

Sohn, H., Park, G., Wait, J. R., Limback, N. P., & Farrar, C. R. (2003). Wavelet-based active sensing for delamination detection in composite structures. IOP Publishing Ltd.

Viktorov I.A. Rayleigh and Lamb Waves, Physical Theory and Applications. *Plenum Press*, New York, 1967.

<div align="center">

VITA
Frank T.J. Sha

</div>

The Air Force Institute of Technology   (626) 384-1932
2950 Hobson Way   E-mail: frank.sha@wpafb.af.mil
Wright-Patterson AFB OH 45433

EDUCATION
2004   Bachelor of Science in Mechanical Engineering, California State Polytechnic University, Pomona CA

ASSIGNMENTS
2010–Present   AFIT Masters Student, Wright Patterson AFB OH
2008–2010   31 FW/CES, Chief of Operations Support, Aviano AB IT
2007–2007   8 FW/CES, Program Manager, Kunsan AB ROK
2004–2007   30 SW/CES, Chief Infrastructure Manager, Vandenberg CA

MAJOR AWARDS AND DECORATIONS
Meritorious Service Medal
Air Force Commendation Medal
Air Force Achievement Medal (2 Devices)
Meritorious Unit Award (1 Devices)
National Defense Service Medal
Afghanistan Campaign Medal (1 Devices)
Iraq Campaign Medal (1 Devices)
Global War On Terrorism Expeditionary Medal
Global War on Terrorism Service Medal
Korean Defense Service Medal
AF Overseas Ribbon Short (1 Devices)
AF Overseas Ribbon Long
Air Force Expeditionary Service Ribbon with Gold Border (1 Devices)
AF Longevity Service
Small Arms Expert Marksmanship Ribbon (Rifle)
AF Training Ribbon
NATO Medal

REPORT DOCUMENTATION PAGE			*Form Approved* OMB No. 074-0188

The public reporting burden for this collection of information is estimated to average 1 hour per response, including the time for reviewing instructions, searching existing data sources, gathering and maintaining the data needed, and completing and reviewing the collection of information. Send comments regarding this burden estimate or any other aspect of the collection of information, including suggestions for reducing this burden to Department of Defense, Washington Headquarters Services, Directorate for Information Operations and Reports (0704-0188), 1215 Jefferson Davis Highway, Suite 1204, Arlington, VA 22202-4302. Respondents should be aware that notwithstanding any other provision of law, no person shall be subject to any penalty for failing to comply with a collection of information if it does not display a currently valid OMB control number.
PLEASE DO NOT RETURN YOUR FORM TO THE ABOVE ADDRESS.

1. REPORT DATE *(DD-MM-YYYY)* 22-03-2012	2. REPORT TYPE Master's Thesis	3. DATES COVERED *(From – To)* Aug 2011 –Mar 2012

4. TITLE AND SUBTITLE Structural Health Monitoring of M1114 High Mobility Multipurpose Wheeled Vehicle Armor System	5a. CONTRACT NUMBER
	5b. GRANT NUMBER
	5c. PROGRAM ELEMENT NUMBER
6. AUTHOR(S) Sha, Frank, T., Capt, USAF	5d. PROJECT NUMBER N/A
	5e. TASK NUMBER
	5f. WORK UNIT NUMBER

7. PERFORMING ORGANIZATION NAMES(S) AND ADDRESS(S) Air Force Institute of Technology Graduate School of Engineering and Management (AFIT/ENV) 2950 Hobson Way, Building 640 WPAFB OH 45433-8865	8. PERFORMING ORGANIZATION REPORT NUMBER AFIT/GEM/ENV/12-M19
9. SPONSORING/MONITORING AGENCY NAME(S) AND ADDRESS(ES) Intentionally left blank	10. SPONSOR/MONITOR'S ACRONYM(S)
	11. SPONSOR/MONITOR'S REPORT NUMBER(S)

12. DISTRIBUTION/AVAILABILITY STATEMENT
  Distribution Statement A. Approved for Public Release; Distribution Unlimited

13. SUPPLEMENTARY NOTES
[The Disclaimer on the second page of your thesis needs to go here!!!]

14. ABSTRACT

Structural Health Monitoring (SHM) is the process of implementing a damage detection and characterization strategy for engineering structures. Damage is defined as changes to the material and geometric properties of a structural system, including changes to the boundary conditions and system connectivity, which adversely affect the system's performance. An active SHM system was developed to detect, locate, and quantify for damage on a two layer composite armor (HJ1 composite with ceramic frontal plates) potentially encountering impact from a 0.30 caliber armor piercing projectile.
An adaptive version of a one at time experimentation was used during this research. Base line testing was completed to understand the individual structural properties and wave propagations characteristics of the materials. Ballistic testing was completed to replicate David Fecko's experimental of maximum V_{50} velocity of 947 meter/second and ceramic to composite ratio of 60/40%. Thus enabling future studies to be completed using data collected from the base line test on to the ballistically tested materials.

15. SUBJECT TERMS
  HJ1, Bulk Longitudinal Waves

16. SECURITY CLASSIFICATION OF:			17. LIMITATION OF ABSTRACT	18. NUMBER OF PAGES	19a. NAME OF RESPONSIBLE PERSON Dr. Som Soni,
a. REPORT U	b. ABSTRACT U	c. THIS PAGE U	UU	106	19b. TELEPHONE NUMBER *(Include area code)* (937) 25-2998, som.soni@afit.edu

Standard Form 298 (Rev. 8-98)
Prescribed by ANSI Std. Z39-18